Suyehiro, K., Sacks, I.S., Acton, G.D., and Oda, M. (Eds.)
Proceedings of the Ocean Drilling Program, Scientific Results Volume 186

9. Tephrochronological and Tephrostratigraphical Potential of Pliocene–Pleistocene Volcaniclastic Deposits in the Japan Forearc, ODP Leg 186[1]

J.B. Hunt[2] and Y.M.R. Najman[3]

ABSTRACT

Major element geochemical composition was established for 59 tephra horizons from Ocean Drilling Program Sites 1150 and 1151, located in the Japan forearc. These data, encompassing typically between 15 and 30 individual shard analyses per tephra horizon, were used to investigate the degree to which sediment reworking, postdepositional geochemical alteration, and geochemical uniqueness of individual eruptives facilitate or impede the potential for establishing a tephrostratigraphical framework for the Japan Trench, as well as usage of the tephra record to document arc evolution. Evidence was found that hydration (termed phase 1 alteration) of glass shards increases with age in the Pliocene–Pleistocene, but there is no indication that element leaching (phase 2 alteration) has occurred. Post- or syn-depositional differences in preservational style are shown to have no significant bearing on tephrogeochemical homogeneity and suitability for tephrostratigraphical analysis. Overall, therefore, the volcaniclastic record is suitable for investigating medium- to long-term changes in arc geochemistry and, provided consideration is given to the potential for nonunique geochemical signatures, is suitable for erecting tephrochronological frameworks. A limited number of Pleistocene tephra correlations are suggested in furtherance of this framework goal.

[1]Hunt, J.B., and Najman, Y.M.R., 2003. Tephrochronological and tephrostratigraphical potential of Pliocene–Pleistocene volcaniclastic deposits in the Japan forearc, ODP Leg 186. *In* Suyehiro, K., Sacks, I.S., Acton, G.D., and Oda, M. (Eds.), *Proc. ODP, Sci. Results,* 186, 1–29 [Online]. Available from World Wide Web: <http://www-odp.tamu.edu/publications/186_SR/VOLUME/CHAPTERS/107.PDF>. [Cited YYYY-MM-DD]
[2]Centre for Environmental Change and Quaternary Research, GEMRU, University of Gloucestershire, Swindon Road, Cheltenham GL50 4AZ, UK.
[3]Department of Geology and Geophysics, University of Edinburgh, West Mains Road, Edinburgh EH9 3JW, UK. **y.najman@glg.ed.ac.uk**

Initial receipt: 2 January 2002
Acceptance: 30 January 2003
Web publication: 27 June 2003
Ms 186SR-107

INTRODUCTION AND PREVIOUS WORK

The volcaniclastic record is key to a number of lines of fundamental research, including documentation of temporal variation in volcanic activity, arc evolution, and stratigraphic correlation. Coring of marine sediments in active tectonic regimes provides opportunities to study the volcaniclastic record more comprehensively than is generally possible in onland studies where exposure is frequently incomplete or poor. However, disadvantages of the marine volcaniclastic record include the potential for sediment reworking and diagenetic alteration. The aims of this current research are (1) to determine the suitability of Leg 186 tephras to the research objectives described above, by documenting levels of diagenetic alteration and reworking to which the tephras, recovered from up to 350 m depth and as old as ~5 Ma, have been subjected; and (2), to provide an indication of the degree of "geochemical uniqueness" of the tephras, required for tephrochronological and tephrostratigraphical purposes (i.e., the degree to which analysis of these tephras provides a readily identifiable geochemical fingerprint). Toward this aim, electron microprobe analyses (EPMA) have been carried out on selected tephras from Japan forearc Sites 1150 and 1151 (Fig. **F1;** Tables **T1, T2;** Tables **AT1, AT2**).

Previous work on tephras offshore from Japan has included much work on the episodic nature of volcanism and its relationship to either global events or regional tectonics (e.g., Cadet and Fujioka, 1980; Arculus et al., 1995; Cambray et al., 1993, 1995) and documentation of tephra geochemistry with the ultimate aims to (1) correlate with the relatively comprehensive onland record (e.g., Pouclet et al., 1986; Furuta et al., 1986; Machida, 1999) and between marine cores (e.g., Fujioka et al., 1980; Furuta and Arai, 1980a, 1980b) and (2) determine arc geochemical evolution (Arculus et al., 1995; Clift et al., in press). All these research objectives are, to a greater or lesser extent, dependent on a volcaniclastic record that is an accurate reflection of onland volcanism, unobscured by secondary marine processes such as diagenesis and reworking. We hope that this work will provide background information that encourages the use of the Leg 186 data set in future studies with the knowledge that the tephras are suitable for these purposes.

TEPHROCHRONOLOGY AND HIGH-PRECISION ANALYSIS

Tephrochronology in its broadest definition is a means of dating or correlating sedimentary signals of (paleo)environmental change. Rapid deposition of tephra on a wide variety of environmental surfaces, including lake beds, mires, soils, ice sheets, and deep and shallow ocean floors, ensures that tephra layers frequently define isochronous surfaces. In the terrestrial Japanese record, widespread tephras have been identified, inter alia, within archaeological horizons, soil horizons, interglacial raised beach deposits, lake sediments, and offshore (see Machida, 1999). Correlation of tephras is frequently heavily reliant upon geochemical analysis of component glass shards that can link tephra, uniquely, to a particular eruption of an identifiable volcano. In this manner tephras may possess a geochemical fingerprint. These geochemical data usually provide the highest degree of certainty that is possible in establishing correlation, particularly where continuous stra-

F1. Sites 1150 and 1151, p. 18.

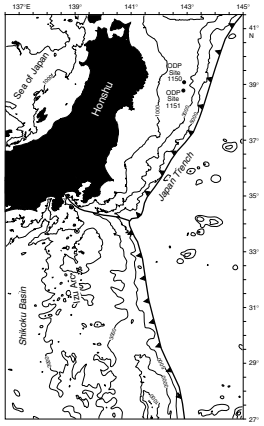

T1. Pliocene–Pleistocene tephra distribution and depositional style, Site 1150, p. 27.

T2. Pliocene–Pleistocene tephra distribution and depositional style, Site 1151, p. 28.

AT1. EPMA of shards from tephra samples, Site 1150, p. 16.

AT2. EPMA of shards from tephra samples, Site 1151, p. 17.

tigraphic mapping is not possible. Firm correlation should only be made, however, where additional independent evidence such as absolute chronology, biostratigraphy, stratigraphical associations, grain size, and mineralogy is shown to be compatible (see Westgate and Gorton, 1981) and where investigations are of sufficient detail and coverage to be confident that discrete geochemical signatures are not shared by multiple eruptives produced hundreds or thousands of years or more apart. This geochemical repetition can be termed geochemical equifinality. Complete confidence in geochemical uniqueness is seldom wholly assured; however, it is highly desirable that its potential is evaluated prior to assigning ages to, or correlating between, analyzed tephras.

This pilot investigation of the tephra record from the Japan Trench focuses on sediments sampled from the Pliocene–Pleistocene sequence (Tables T1, T2) to evaluate the effects of alteration, broad geochemical changes, and the potential influence of differing modes of preservational style on the tephra record. At this initial stage, the criteria outlined above and required for rigorous tephrostratigraphical correlation have not been adhered to but await more detailed investigation. Therefore, this research cannot and should not be used to erect a chronological framework for the Pliocene–Pleistocene. It may be possible to suggest potential correlation to tephra isochrons defined in earlier studies, but these correlations must be treated with caution.

ANALYTICAL METHODOLOGY

Geochemical techniques reliant upon bulk sample analysis are generally not thought suitable for tephrochronological purposes, albeit that they may satisfy petrological requirements to characterize geochemical provinces. Grain discrete methods are required in order that detrital contamination or the variable influence of (micro)phenocryst phases can be excluded. EPMA is the most widely applied of the grain discrete techniques and is adapted to analyze the principal glassy phases of tephra in order to determine the most subtle geochemical differences both between the products of individual volcanic centers and of discrete eruptions within those centers.

The geochemical study of tephra by EPMA has afforded considerable advances in tephrochronological studies and remains the principal means of characterizing major element tephrogeochemistry of glass shards. The method is, however, not without its problems; the most significant of these for tephrochronology is the deleterious effect of the probe's electron beam in inducing alkali metal mobility within the matrix of the glass shards. This effect has been outlined and detailed by many authors both in natural and synthetic glasses (Keller, 1981; Nielsen and Sigurdsson, 1981; Hunt and Hill, 1993) and in albite (Autefage and Couderc, 1980). The most significant effect of this mobility, if inappropriate analytical conditions are utilized, is the apparent loss of sodium from the sample. In terms of the final geochemical quantitation, the tephra will appear to have low Na_2O concentrations and slightly elevated SiO_2 and Al_2O_3 concentrations. As the analytical conditions that impose these effects are commonly employed in standard petrological analysis, it is unsurprising that there are numerous examples of erroneous analyses in the literature. These have been explored by Hunt and Hill (1994, 1996) and Hunt et al. (1998). Given that the severity of the potential impact of poor analysis includes incorrect attri-

bution of tephras to volcanic regions (Hunt and Hill, 2001) and potential confusion of key tephra isochrons, great care is required in adopting appropriate analytical conditions.

Geochemical analyses of tephras in this paper were performed by wavelength dispersive spectrometry (WDS) on a Cambridge Instruments Microscan V, under the following conditions: accelerating voltage = 20 kV, beam current = 15 nA (measured by Faraday Cup), peak count per element = 10 s, and a defocused (5–10 μm) beam. Na_2O and SiO_2 concentrations were determined first to minimize the effects described above. The knock-on effects of Na_2O mobility on remaining elements, later in each analysis, were minimized by blanking the electron beam during spectrometer repositioning and reducing the electron beam exposure time to 50 s. Both oxides and simple silicates were used as standards. Corrections were made for counter dead time, atomic number (*Z*) effects, fluorescence (*F*), and absorption (*A*) using a ZAF procedure described by Sweatman and Long (1969). Andradite garnet and Lipari obsidian (Hunt and Hill, 1996) were employed as secondary standards to assess for stability of beam and reliability of glass data. These analyses are available on request. WDS data are found to be of much higher precision than those obtained through energy dispersive spectrometry (EDS) as demonstrated, inter alia, by Hunt and Hill (1996). As a consequence of this rigorous approach, we are confident that the analyses (Tables **AT1, AT2**) reflect the best possible data that can be obtained from tephras in the Japanese marine record, although we recognize that the data set could have been further enhanced by determination of volatiles (fluorine and chlorine) and minor elements (e.g., phosphorus).

DEPOSITIONAL STYLE: LAYERS, PODS, AND PUMICES

Shipboard classification of primary volcanigenic sediments encompassed three principal groups: pumices, pods, and layers (Sacks, Suyehiro, Acton, et al., 2000). In this initial study we have excluded pumice analysis, principally because, although pumices may be deposited shortly after their eruption, they may equally drift or reside in the environment to be deposited/transported many thousands of years later (e.g., see Binns, 1972; Newton and Dugmore, 1995; Bryan, 1968). However, this does present some problems in attempting to establish a tephrostratigraphic correlation with the terrestrial record, as some eruptions may be represented in more distal marine deposits by pumice alone.

The process of pod formation is not clear. Cambray et al. (1993) suggest that pods in the Pacific Ocean are formed by the disruption of thin layers of tephra by the burrowing action of benthic dwellers such as *Zoophycos* and *Phonolites*. In this mode of pod formation, geochemical integrity of the reworked tephra is likely to be maintained, albeit the proportion of nonvolcanigenic grains may be reduced by dilution. An additional pod formation process whereby strong currents and steep bottom topography play a role in controlling the tephra form has been proposed by Fujioka (1986). If such formation occurs while the tephra remains exposed on the seafloor, its stratigraphical context is not lost and its geochemical characteristics are preserved, albeit with potential dilution of the volcanigenic content. If, however, tephra redistribution by bottom-current/turbidite activity occurs after burial, the potential

stratigraphic significance may be lost, as such large-scale reworking processes are likely to concentrate the products of more than one eruption. This reworking process, which can affect tephra layers as well as pods, will result in decreased homogeneity of the unit compared to a primary deposit. In light of these uncertainties, there is some debate regarding the usage of pods, especially their inclusion in the recording of the frequency of volcanic activity, with some workers discounting pods entirely (see discussion in Cadet and Fujioka, 1980). If the pods are to be used as reliable stratigraphical markers, they must have the same likelihood as layers of representing the products of only one eruption. It follows from these assertions that for the layers and pods to function as tephra marker horizons, their geochemistry should be either (1) well-trended (i.e., displaying a clear fractionation/evolution signal) or (2) relatively homogeneous, with no significant difference in homogeneity between pods and layers.

Leg 186 shipboard smear slide data (Sacks, Suyehiro, Acton, et al., 2000) show that none of the pods contain >85% vitric shards in their total framework composition, whereas 50% of layers do (Fig. **F2;** Table **T3**). This contrasts with smear slide data from tephras from nearby Deep Sea Drilling Project (DSDP) Leg 57, where 25% of both layers and pods contain >85% vitric shards (Fujioka et al., 1980); homogeneity indices may be a more robust indicator of the suitability of pods for tephrochronological purposes. Homogeneity indices have been proposed (Boyd et al., 1967; Potts et al., 1983) for investigating the "quality" of potential analytical standards. Both of these methods, however, require reference to instrumental counting statistics and are not readily applicable to published data. We have therefore taken the more straightforward, but nonetheless valid, approach of comparing standard deviations of key major elements (Si, Al, K, and Na) for all analyses of each layer/pod. We observed no significant difference between the standard deviations (i.e., homogeneity) of layers and pods (Fig. **F3**). We conclude, therefore, that layers and pods can be regarded equally in terms of their tephrostratigraphic utility and that pod formation occurs without introducing substantial allochthonous volcanic and nonvolcanic components. From these data however, we cannot comment on the relative merits of the biogenic and current-driven redistribution models that have been used to explain pod formation. In general, the tephra units analyzed in this study are well clustered, indicative of good homogeneity and encouraging for their potential tephrochronological utility, as demonstrated in the later section on geochemistry and correlations.

TEMPORAL TRENDS IN GEOCHEMICAL ALTERATION

Coring at Ocean Drilling Program (ODP) Sites 1150 and 1151 has yielded the most complete recovery of Pliocene–Pleistocene marine tephras that has yet been obtained in the Japan Trench. As such, they provide the opportunity to study the effects of age on tephra geochemistry, not only as a function of temporal changes in magma composition but as influenced by postdepositional chemical alteration of glass shards. As the geochemical signature of glass shards can be moderated by medium to high degrees of postdepositional weathering, this deep record of volcanic history provides a useful opportunity to assess alteration trends and thereby the reliability of geochemical tephra correla-

F2. Volcaniclastic components in tephra pods and layers, p. 19.

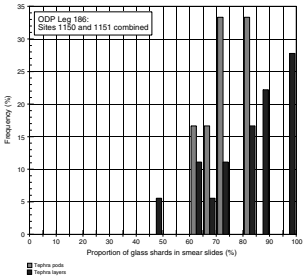

T3. Proportions of volcanic material in tephra layers and pods, p. 29.

F3. Major element oxides from shards in tephra layers and pods, p. 20.

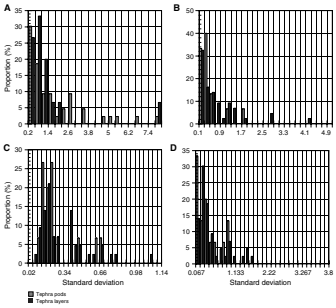

tions for the entire Quaternary and earlier. This parallels similar work by Masuda et al. (1993) in the Nankai Trough.

The geochemical instability of glass has been noted and assessed in a variety of environments (Fisher and Schmincke, 1984; Jezek and Noble, 1977). The stages and chemomechanics of hydration and subsequent devitrification are complex and poorly understood, although the progress from unweathered glass through perlite (hydrated glass-obsidian) to microcrystallite clay mineral growth and ultimate zeolitization is fundamentally a two-stage process. The first phase is the addition of water into the glass matrix. This proceeds at varying rates, dependent upon environment, glass chemistry, and temperature. Compared with basaltic glass (sideromelane), alteration of silicic glass initially involves little solid-state change (Fisher and Schmincke, 1984) as water is taken up by the glass "matrix" (Friedman and Long, 1976). At this stage, up to 3% water can be held in the glass (Friedman and Smith, 1958; Jezek and Noble, 1977; Hunt and Hill, 1993) with low ion exchange. Additional hydration subsequently takes place, initially along fracture surfaces, resulting in the "weakening and breakage of the bonds of the glass structure" (Jezek and Noble, 1977) with a tendency for clay and zeolite mineral growth during phase 2.

The initial hydration process does not result in significant ion mobility across the entire compositional range of the glass, but Na_2O and K_2O are particularly mobile, with a depletion of K_2O and an enhancement of Na_2O (Jezek and Noble, 1977). Hydration of glasses has been monitored by EPMA studies (Jezek and Noble, 1977) to demonstrate the direct (albeit nonlinear) relationship between water content and analytical (oxide sum) totals. Application of this simple relationship to glasses (shards) of different ages but in similar depositional settings can be used to investigate temporal variations in glass alteration. This has been attempted in this study of Leg 186 tephras, of which the analyzed shards span an interval of ~0–5 Ma. This age range and the relatively low geothermal gradient (Sacks, Suyehiro, Acton, et al., 2000) suggest that these tephras will lend themselves particularly well to investigation of the impact of phase 1 (i.e., hydration only) alteration.

Age-alteration relationships are investigated through depth vs. total oxide plots (Fig. **F4**). At present, age models lack the robustness to convert all depths to specific ages since currently details of the age-depth model for holes drilled during Leg 186 are unresolved (Sacks, Suyehiro, Acton, et al., 2000; **Hayashi et al.; Li; Maruyama and Shiono,** all this volume). Therefore, at this stage we feel that interpretations which utilize anything other than *broadly* indicative age-depth information would be premature. The total oxides data display considerable scatter, which may reflect (1) varying proportions of undetermined volatiles other than water (e.g., fluoride and chloride), (2) varying proportions of undetermined primary water, (3) varying susceptibility to phase 1 alteration as a result of varying vesicularity or shard size (e.g., Cambray et al., 1993; Dugmore et al., 1995), or (4) variability of host sediment porosity and pore water supply. However, this variability between layers is superimposed on a clear age trend, particularly apparent in the more extensive (to ~350 meters below seafloor [mbsf]) record from Site 1151. Nevertheless, although an age/depth–driven alteration trend is apparent, its magnitude over the Pliocene–Pleistocene is sufficiently small that judicious tephrostratigraphical correlation may be achieved, albeit with caution if attempts are made to link with terrestrial sites with different weathering/diagenetic regimes. Of additional interest is the ab-

F4. Decrease of total oxides in the tephra, p. 21.

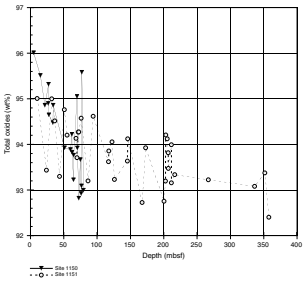

sence of an age trend related to Al_2O_3/SiO_2 ratios. Masuda et al. (1993) suggest that the Al_2O_3/SiO_2 ratio is an index of marine burial diagenesis, due to the preferential solubility of Si relative to Al. Our data show no such change with depth (Fig. F5), implying relative geochemical resistance to alteration over Pliocene–Pleistocene timescales. From these observations we can conclude that changes have occurred over time through the addition of water to the glass "matrix," but that this addition has not yet been accompanied by geochemical breakdown through selective leaching of elements from the glass matrix. Our findings are broadly in agreement with those of Arthur et al. (1980), Cadet and Fujioka (1980), Fujioka (1986), and Fujioka et al. (1980), who show that alteration is only minimal at equivalent ages and depths at nearby DSDP Sites 56, 57, and 87B. These results are relatively encouraging for Pliocene–Pleistocene marine tephrochronology in the Japan Trench.

The maximum sample depth of tephra analyzed in this study (Site 1151) is 357 mbsf (age = ~4.9 Ma), where the overall geothermal temperature gradient is 27.7°C/km (Scientific Party, 1980). This gradient accords well with the Site 1150 data (for the upper 155 mbsf, temperature gradient = 28.9°C/km) but contrasts significantly with results from the nearby Nankai Trough (ODP Leg 131), where the geothermal gradient exceeded 111°C/km (Masuda et al., 1993). Despite this significantly greater heat flux, Masuda et al. (1993) report no significant ash alteration in the upper 500 mbsf. This is perhaps surprising, given the general consensus that geothermal gradient is the primary control on tephra alteration (see Hein and Scholl, 1978; Grechin et al., 1980; Cambray et al., 1993). This difference in reported weathering may reflect differing analytical approaches (e.g., bulk vs. grain discrete) or, more likely, may be due to the concentration of prior studies on phase 2 alteration processes contrasted by this study of Pliocene–Pleistocene tephras.

F5. Lack of time-dependent signal in Al_2O_3/SiO_2 ratios, p. 22.

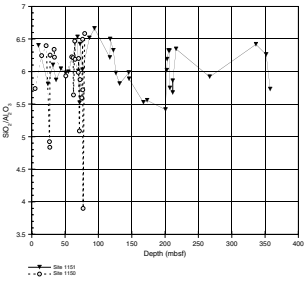

TEMPORAL DISTRIBUTION OF VOLCANIC ASH

The potential causes of temporal changes in volcanic activity in many of the world's volcanic regions are varied and have been the subject of considerable debate (e.g., Matthews, 1969; Kennett and Thunnell, 1977; Grove, 1976; Hein et al., 1978; Rampino et al., 1979; Donn and Ninkovich, 1980; Hall, 1982; Fujioka, 1986; Hardarson and Fitton, 1991; Sigvaldason et al., 1992). The suggestion of causal links between volcanic activity and climatic change is widely upheld. Commonplace is the suggestion that volcanism, by the emission of eruptive gases, induces climate change (Lamb, 1970). Additionally, many workers have indicated, through the effects of glacio- or hydro-isostasy (loading and unloading), that climatic cycles may control volcanic activity (Kennett and Thunnell, 1977; Rampino et al., 1979; McGuire et al., 1997; Sigvaldason et al., 1992). Other workers have suggested that changes in the global rates of volcanic activity are linked to changing activity of the global tectonic system, for example, changes in oceanic spreading rates (Kennett and Thunnell, 1977).

It follows that ongoing assessment of rates of volcanic activity will form a crucial component of this debate, particularly where (1) data are gathered from the continuously accumulating sediments around key volcanic regions and (2) advanced coring methods lead to more complete recovery of the sedimentary record. The effects of variable core recovery on the statistical validity of age–eruption frequency models are

discussed by Sigurdsson and Loebner (1981). Although the Pleistocene recovery is generally very good for Leg 186 sites, especially Hole 1150A, sediment loss at depth is not insignificant (Hole 1150A: recovery = 73% from 112 to 722 mbsf; Hole 1151A: recovery = 68% from 78 to 1113 mbsf). This discontinuous recovery hinders evaluation of eruption frequency variations in the pre-~1-Ma record. In addition, a reliable and generally accepted age model for Sites 1150 and 1151 is required before such evaluation and comparison with other sites (see Cadet and Fujioka, 1980; Fujioka, 1986; Cambray et al., 1993) can be attempted.

GEOCHEMISTRY AND CORRELATIONS

Tephra geochemistry has been established for selected Pliocene–Pleistocene tephras from both Leg 186 Sites (1150 and 1151). These have been compared with published data for named/previously identified tephras both on land and in the marine record from the Japan region (Cadet and Fujioka, 1980; Fujioka et al., 1980; Furuta and Arai, 1980a, 1980b; Machida, 1999; Machida et al., 1984, 1985, 1987; Pouclet et al., 1986). As the majority of previously characterized tephras are principally found in the Quaternary record (see Machida, 1999), we have confined our discussion of potential correlations to the Pleistocene succession.

The data considered in this study comprise multiple electron probe analyses of tephric glass shards. Although the Atlas of Japanese Tephrochronology (Machida and Arai, 1992) presents multiple analyses from discrete tephras, difficulties arise in comparing tephrogeochemistry from our study with many published data sets, principally due to a widespread tendency to publish single mean data points and standard deviations rather than representative individual analyses (e.g., Machida, 1999). This difficulty is compounded further by the publication of normalized data without an indication of assumed volatile (including water) content—thereby losing an indication of (1) the potential effects of alkali metal mobility (loss) and (2) the effective enhancement of the higher-abundance element oxides (e.g., silica and alumina). An additional source of difficulty arises in drawing comparisons with Japanese tephrochronological data that are based on tephra characterization by refractive index (RI) of glass shards. Where only RI data are available, comparison between many onland Japanese tephra is often problematic, as ODP/DSDP tephra studies are frequently based on EPMA data alone. As RI is based on the density of the glass, it is *possible* that any single range of RI values could arise through two or probably many more discrete geochemical compositions; Furuta et al. (1986) suggest that the transition metal (and particularly ferric and ferrous) oxides control RI. Additionally, the effects of variable shard hydration on RI values must be considered. These factors *appear*, initially, to suggest that EPMA data for shard geochemistry may have greater utility in distinguishing and correlating tephras than RI methods. Therefore, if the RI approach is to gain international acceptance, a widely disseminated rigorous comparative exercise is required between RI and EPMA data sets. The work of Furuta and Arai (1980a, 1980b) and Furuta et al. (1986) begins to address this issue, but their results (see Furuta et al., 1986, p. 140, fig. 6), from a limited number of tephras, can be interpreted as indicating greater problems with RI as a tool in tephra correlation, particularly compared with EPMA.

In different volcanic regions, particular element pairs determined by EPMA prove useful in distinguishing between tephras produced from the same or different eruptive centers. In Iceland, for example, FeO/CaO ratios and FeO/TiO_2 ratios are frequently the most useful indices for identifying particular tephras. In Japan one of the most useful oxide pairs in this approach is TiO_2/K_2O (see Machida et al., 1987), although additional examination, in particular of MgO, FeO, and CaO, offers further assistance. In attempting to establish tephra correlations, all major elements have been examined from readily available published data and our own extensive analysis of Leg 186 tephras. For each of the 59 tephras whose geochemical compositions are reported herein (see Tables **AT1, AT2**), up to 30 individual shards have been analyzed. A minimum number of 15 analyses was sought and where this was not achieved it reflects the number of shards exposed on the probe slide surface and available to the electron beam. Data that clearly reflect sample damage during analysis, with subsequent low totals, have been removed. This problem is particularly acute in highly vesicular (pumiceous) thin-walled shards.

SITE 1151

EPMA data for 36 individual tephras (layers and pods) were analyzed from Site 1151 (Tables **T2, AT2**), spanning an age interval, suggested by original shipboard age estimations, of ~130 ka to 4.8 Ma. Data for tephras younger than ~2.25 Ma are presented in Figure **F6.** Tephrogeochemical populations are generally well clustered in terms of individual element oxides, which is encouraging in terms of their tephrochronological utility; tephras from Samples 186-1151C-2H-6, 42–44 cm, through 9H-1, 14–16 cm, for example, all plot discretely in terms of TiO_2 and K_2O. However, as the data set expands, geochemical equifinality becomes apparent, with shared geochemical fingerprints arising between tephra Samples 186-1151C-9H-1, 14–16 cm, and 186-1151A-7R-1, 35–37 cm, 186-1151C-2H-6, 42–44 cm, and 186-1151A-6R-4, 26–28 cm; and 186-1151C-5H-4, 145–146 cm, and 9H-5, 143–145 cm (Fig. **F6**). This is likely to be a greater problem than we have currently identified because of our partial sampling of the Neogene tephra record. Where major element geochemistry is insufficient to characterize a tephra uniquely, additional geochemical data may prove helpful (e.g., trace element characterization by laser ablation–inductively coupled plasma mass spectrometry [ICP-MS], e.g., Bryant et al. [1999], Pearce et al. [1999]). Failing this, additional stratigraphic or geochronological evidence such as marine isotope stage (MIS) characterization is required. Currently available age models lack the robustness to facilitate correlation with MIS stratigraphy determined in the Japan region. Despite the large, albeit incomplete, number of tephras analyzed from Site 1151, we are unable to propose a single specific correlation, either with the tephra record of Site 1150 or with the onland or regional marine tephrostratigraphy. The lack of correlation between sites is particularly surprising, given their relative proximity. Potential explanatory factors that require further exploration include (1) localized variation in bottom-current activity and zones of sediment movement and deposition and (2) possible hiatuses in the upper parts of the Site 1151 record.

F6. EPMA data for tephras, p. 23.

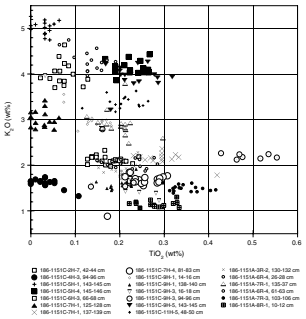

SITE 1150

EPMA data for 23 individual tephras (layers and pods) were obtained from Site 1150 (Tables T1, AT1), spanning an age interval, suggested by original shipboard age estimations, of ~24 to 665 ka. On the basis of major element geochemical composition it is possible to suggest two correlations between Site 1150 tephras and previously described isochrons.

First, tephra Sample 186-1150A-2H-5,136–138 cm, appears to correlate (Fig. F7) with the ~40-ka SpFa-1 tephra erupted from the Shikotsu caldera in Hokkaido (Machida, 1999). This tephra has been reported in the Pacific Ocean, offshore from Hokkaido and Northeast Honshu. Confirmation of this correlation would extend the known range of this deposit farther to the south. Correlation with the 20-ka Aira-Tn tephra, supported by TiO_2/MgO ratios, can be rejected because of significant differences in K_2O. Acceptance of the correlation with tephra SpFa-1 would indicate that the original ship-based age model (74 ka) had overestimated the age for this depth (15.06 mbsf) by ~30 k.y.

Second, tephra Sample 186-1150A-4H-1, 10–12 cm (and duplicated in core catcher Sample 3H-CC, 22–25 cm), appears to correlate with the Aso-4 tephra, erupted at ~84–89 ka from the Aso caldera (Machida and Arai, 1992; Machida et al., 1985). The Aso-4 tephra represents the youngest and largest of the Aso eruptions and one of the largest Japanese eruptions of the middle to late Quaternary. Geochemically, it has a distinct bimodality, and despite the many caveats expressed in this paper concerning the potential for geochemical equifinality and for miscorrelation, we can be reasonably confident in this correlation, supported by TiO_2/K_2O, FeO/MgO, and SiO_2/CaO ratios (Fig. F8). Acceptance of the correlation with the Aso-4 tephra would indicate that the original ship-based age model (~130 ka) had overestimated the age for this depth (26.8 mbsf) by ~45 k.y. It is of interest to those with specific interest in high-resolution stratigraphic investigations from ODP cores to note the evidence of core overlap that this tephra provides. Both samples (186-1150A-4H-1, 10–12 cm, and 3H-CC, 22–25 cm) are clearly from the same real depth, as indicated by the tephra layer. The core catcher (186-1150A-3H-CC) tephra sample is assigned a depth of 27.27 mbsf by coring protocol and the tephra from the lower core (186-1150A-4H) a depth of 26.8 mbsf. As the geochemical evidence is not readily contradicted, one is forced to assume that Cores 186-1150A-3H and 4H overlapped by 47 cm. Whereas this may not be of significance in terms of long-term shifts, those investigating high-resolution paleoceanographic and paleoclimatic shifts from ODP piston cores should be mindful of this issue, which will only be revealed in the rare instances where marker horizons are present and confirmed as such (see also Robinson, 1990).

Although these are the only widespread terrestrial and marine tephras that we have suggested may potentially correlate with Site 1150 tephras, there may be further correlative potential with additional tephras in the Japan region, including both Holocene and Pleistocene deposits. Finally, for Site 1150, one tephra layer (Sample 186-1150A-9H-3, 2–4 cm) is, in comparison with the dominantly rhyolitic tephras from Sites 1151 and 1150 and the Quaternary terrestrial record, uncharacteristically andesitic to dacitic (Fig. F9). This tephra, dated by the original shipboard age models to ~660 ka, appears to correlate (Fig. F9) with dacitic and andesitic tephras defined by Pouclet et al. (1986) from Holes

F7. Comparison between late Quaternary tephras, p. 24.

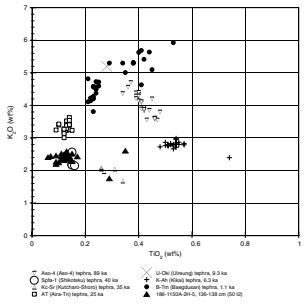

F8. Comparison between Hole 1150A tephras and Japanese tephras, p. 25.

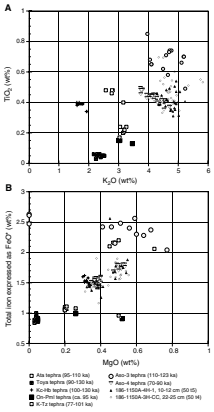

F9. Comparison of tephras, p. 26.

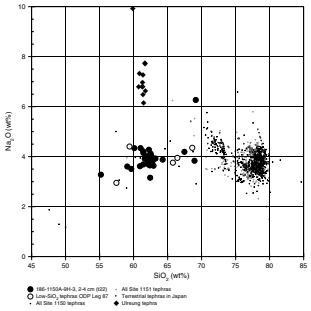

582B, 583A, and 583D (their samples 9, 10, 27, and 29) from Leg 87. These are of undetermined Quaternary age. Whether tephra Sample 186-1150A-9H-3, 2–4 cm, is correlative with one of these is unclear, albeit a distinct possibility.

CONCLUSIONS

In this initial study of the Japan Trench volcaniclastic sediments, we have attempted to ascertain the potential of the Pliocene–Pleistocene tephras to provide a tephrochronological framework for the Japan area and a record of arc evolution. This approach reflects global developments (e.g., see Lowe, 1996; Hunt, 1999) that are using high-precision tephrostratigrapical studies to refine our knowledge of the chronology of environmental change and the linkages between marine and terrestrial geosystems. We draw the following conclusions in relation to the Japan Trench tephras.

1. Although there is convincing evidence that hydration (phase 1 alteration) of glass shards increases with age in the Pliocene–Pleistocene, there is no indication that element leaching (phase 2 alteration) has occurred. Provided that inter-environmental differences in hydration rates are considered, the potential for correlation with tephras elsewhere is not hindered by pervasive diagenesis during Pliocene–Pleistocene times.
2. There are no differences in the geochemical homogeneity of glass shard populations in pods and layers. The use of tephra pods as potential stratigraphical markers is therefore possible.
3. Despite high-precision analysis of glass shards, it is in some instances not possible to distinguish geochemical differences between tephras (eruptions). This presents problems in the marine record where the low number of coring sites and the inability to perform "hand-over-hand" lateral correlations between closely spaced sites prevents unambiguous tephra correlation. Therefore, correlation of tephra layers cannot be achieved by geochemical fingerprinting alone but requires systematic high-resolution stratigraphical and geochemical analysis of all visible and *crypto*- tephra layers and/or independent geochronological data in parallel with the tephrostratigraphy.
4. The relatively high recovery of Pleistocene sediments can permit, for the first time, a near-continuous temporal record downwind from centers of explosive volcanism on Honshu in particular and the Japan arc in general. An age model that accords with generally accepted bio- and magnetostratigraphy is, however, required before this can be achieved. We maintain that tephrochronology should not be a critical input to this model, unless all tephras in a particular record have been analyzed.
5. The general homogeneity of the pods and layers and the relatively nonpervasive alteration suggests that the volcaniclastic record of the Japan Trench is suitable for further geochemical investigations of arc evolution.

ACKNOWLEDGMENTS

This research used samples provided by the Ocean Drilling Program (ODP). The ODP is sponsored by the U.S. National Science Foundation (NSF) and participating countries (including the UK) under management of Joint Oceanographic Institutions (JOI), Inc. Funding for this research was provided by the Natural Environment Research Council, the Royal Society, and the Royal Society of Edinburgh to Y.N.

REFERENCES

Arculus, R.J., Gill, J.B., Cambray, H., Chen, W., and Stern, R.J., 1995. Geochemical evolution of arc systems in the western Pacific: the ash and turbidite record recovered by drilling. *In* Taylor, B., and Natland, J. (Eds.), *Active Margins and Marginal Basins of the Western Pacific*. Am. Geophys. Union, 88:45–65.

Arthur, M.A., von Huene, R., and Adelseck, C.G., Jr., 1980. Sedimentary evolution of the Japan forearc region off northern Honshu, Legs 56 and 57, Deep Sea Drilling Project. *In* Scientific Party, *Init. Repts. DSDP,* 56, 57 (Pt. 1): Washington (U.S. Govt. Printing Office), 521–568.

Autefage, F., and Couderc, J.-J., 1980. Étude du mécanisme de la migration du sodium et du potassium au cours du leur analyse a la microsonde électronique. *Bull. Mineral.,* 103:623–629.

Binns, R.E., 1972. Composition and derivation of pumice on post glacial strandlines in northern Europe and the western Arctic. *Geol. Soc. Am. Bull.,* 83:2303–2324.

Boyd, F.R., Finger, L.W., and Chayes, F., 1967. Computer reduction of electron-probe data. *Yearbook—Carnegie Inst. Washington,* 67:210–215.

Bryan, W.B., 1968. Low-potash drift pumice from the Coral Sea. *Geol. Mag.,* 105:431–439.

Bryant, C.J., Arculus, R.J., and Eggins, S.M., 1999. Laser ablation-inductively coupled plasma–mass spectrometry and tephras: a new approach to understanding arc-magmas genesis. *Geology,* 27:1119–1122.

Cadet, J.-P., and Fujioka, K., 1980. Neogene volcanic ashes and explosive volcanism: Japan Trench transect, Leg 57, Deep Sea Drilling Project. *In* Scientific Party, *Init. Repts. DSDP,* 56, 57 (Pt. 2): Washington (U.S. Govt. Printing Office), 1027–1041.

Cambray, H., Cadet, J.-P., and Pouclet, A., 1993. Ash layers in deep-sea sediments as tracers of arc volcanic activity: Japan and Central America as case studies. *The Island. Arc,* 2:72–86.

Cambray, H., Pubellier, M., Jolivet, L., and Pouclet, A., 1995. Volcanic activity recorded in deep-sea sediments and the geodynamic evolution of western Pacific island arcs. *In* Taylor, B., and Natland, J. (Eds.), *Active Margins and Marginal Basins of the Western Pacific*. Geophys. Monogr., Am. Geophys. Union, 88:97–124.

Clift, P.D., Layne, G.D., Shimizu, N., Kopf, A., and Najman, Y., 2002. Temporal evolution of boron flux in the Izu and Honshu arcs measured by ion microprobe from the forearc tephra record. *Eos Trans., Am. Geophys. Union,* 83:T72A–1235.

Donn, W.L., and Ninkovich, D., 1980. Rate of Cenozoic explosive volcanism in the North Atlantic Ocean inferred from deep sea cores. *J. Geophys. Res.,* 85:5455–5460.

Dugmore, A.J., Larsen, G., and Newton, A.J., 1995. Seven tephra isochrones in Scotland. *The Holocene,* 5:257–266.

Fisher, R.V., and Schmincke, H.-U., 1984. *Pyroclastic Rocks:* New York (Springer-Verlag).

Friedman, I., and Long, W., 1976. Hydration rate of obsidian. *Science*, 191:347–352.

Friedman, I., and Smith, R.L., 1958. The deuterium content of water in some volcanic glasses. *Geochim. Cosmochim. Acta*, 15:218–228.

Fujioka, K., 1986. Synthesis of Neogene explosive volcanism of the Tohoku arc, deduced from marine tephra drilled around the Japan Trench region, Deep Sea Drilling Project Legs 56, 57, and 87B. *In* Kagami, H., Karig, D.E., Coulbourn, W.T., et al., *Init. Repts. DSDP,* 87: Washington (U.S. Govt. Printing Office), 703–726.

Fujioka, K., Furuta, T., and Arai, F., 1980. Petrography and geochemistry of volcanic glass: Leg 57, Deep Sea Drilling Project. *In* von Huene, R., Nasu, N., et al., *Init. Repts. DSDP,* 56, 57 (Pt. 2): Washington (U.S. Govt. Printing Office), 1049–1066.

Furuta, T., and Arai, F., 1980a. Petrographic and geochemical properties of tephras in Deep Sea Drilling project cores from the North Philippine Sea. *In* Klein, G. deV., Kobayashi, K., et al., *Init. Repts. DSDP,* 58: Washington (U.S. Govt. Printing Office), 617–625.

Furuta, T., and Arai, F., 1980b. Petrographic properties of tephras, Leg 56, Deep Sea Drilling Project. *In* von Huene, R., Nasu, N., et al., *Init. Repts. DSDP,* 56, 57 (Pt. 2): Washington (U.S. Govt. Printing Office), 1043–1048.

Furuta, T., Fujioka, K., and Arai, F., 1986. Widespread submarine tephra around Japan, petrographic and chemical property. *Mar. Geol.,* 72:125–146.

Grechin, V.I., Neim, A.R., Mahood, R.O., Alexandrova, V.A., and Sakharov, B.A., 1980. Neogene tuffs, ashes and volcanic breccias from offshore California, DSDP, Leg 63: sedimentation and diagenesis. *Init. Repts. DSDP,* 63: Washington (U.S. Govt. Printing Office), 631–657.

Grove, E.W., 1976. Deglaciation—a possible triggering mechanism for recent volcanism. *In* Ferran, O.G. (Ed.), *Proceedings of the Symposium on Andean and Antarctic Volcanology Problems, Santiago, Chile, September 1974.* Int. Assoc. Volcanol. Chem. Earth's Interior, Spec. Ser., 1–10.

Hall, K.J., 1982. Rapid deglaciation as an initiator of volcanic activity: an hypothesis. *Earth Surf. Processes Landforms,* 7:45–51.

Hardarson, B.S., and Fitton, J.G., 1991. Increased mantle melting beneath Snaefellsjökull volcano during Late Pleistocene deglaciation. *Nature,* 353:62–64.

Hein, J.R., and Scholl, D.W., 1978. Diagenesis and distribution of late Cenozoic volcanic sediment in the southern Bering Sea. *Geol. Soc. Am. Bull.,* 89:197–210.

Hein, J.R., Scholl, D.W., and Miller, J., 1978. Episodes of Aleutian Ridge explosive volcanism. *Science,* 199:137–141.

Hunt, J.B. (Ed.), 1999. Distal tephrochronology, tephrology, and volcano-related atmospheric effects. *Global Planet. Change,* 21:1–196.

Hunt, J.B., Clift, P.D., Lacasse, C., Vallier, T.L., and Werner, R., 1998. Interlaboratory comparison of electron probe microanalysis of glass geochemistry. *In* Saunders, A.D., Larsen, H.C., and Wise, S.W., Jr. (Eds.), *Proc. ODP, Sci. Results,* 152: College Station, TX (Ocean Drilling Program), 85–91.

Hunt, J.B., and Hill, P.G., 1993. Tephra geochemistry: a discussion of some persistent analytical problems. *The Holocene,* 3:271–278.

————, 1994. Geochemical data in tephrochronology: a reply to Bennett. *The Holocene,* 4:436–438.

————, 1996. An interlaboratory comparison of the electron probe microanalysis of glass geochemistry. *Quat. Int.,* 35/36:221–224.

————, 2001. Tephrological implications of beam size—sample size effects in electron microprobe analysis of glass shards. *J. Quat. Sci.,* 16:105–117.

Jezek, P.A., and Noble, D.C., 1977. Natural hydration and ion exchange of obsidian: an electron microprobe study. *Am. Mineral.*, 63:266–273.

Keller, J., 1981. Quaternary tephrochronology in the Mediterranean. *In* Self, S., and Sparks, R.S.J. (Eds.), *Tephra Studies:* Dordrecht (D. Reidel), 227–244.

Kennett, J.P., and Thunnell, R.C., 1977. On explosive Cenozoic volcanism and climatic implications. *Science,* 196:1231–1234.

Lamb, H.H., 1970. Volcanic dust in the atmosphere; with a chronology and assessment of its meteorological significance. *Philos. Trans. R. Soc. London, Ser. A,* 266:425–533.

Lowe, D.J. (Ed.), 1996. Tephra, loess, and paleosols—an integration. *Quat. Int.,* 34/36:1–261.

Machida, H., 1999. The stratigraphy, chronology and distribution of distal marker-tephras in and around Japan. *Global Planet. Change,* 21:71–94.

Machida, H., and Arai, F., 1992. *Atlas of Tephra in and around Japan*. Tokyo (Tokyo Univ. Press).

Machida, H., Arai, F., Lee, B.S., Moriwaki, H., and Furuta, T., 1984. Late Quaternary tephras in Ulreung-do Island, Korea. *J. Geogr. Japan,* 93:1–14.

Machida, H., Arai, F., Miyauchi, T., and Okumura, K., 1987. Toya ash—a widespread tephra and its implications for late Pleistocene events in and around Japan. *Bull. Volcanol. Soc. Japan,* 30:49–70.

Machida, H., Arai, F., and Momose, M., 1985. Aso-4—a widespread late Quaternary time-marker in northern Japan. *Quat. Res.,* 26:129–145.

Masuda, H., Tanaka, H., Gamo, T., Soh, W., and Taira, A., 1993. Major-element chemistry and alteration mineralogy of volcanic ash, Site 808 in the Nankai Trough. *In* Hill, I.A., Taira, A., Firth, J.V., et al., *Proc. ODP, Sci. Results,* 131: College Station, TX (Ocean Drilling Program), 175–183.

Matthews, R.K., 1969. Tectonic implications of glacio-eustatic sea level fluctuations. *Earth Planet. Sci. Lett.*, 5:459–462.

McGuire, W.J., Howarth, R.J., Firth, C.R., Solow, A.R., Pullen, A.D., Saunders, S.J., Stewart, I.S., and Vita-Finzi, C., 1997. Correlation between rate of sea-level change and frequency of explosive volcanism in the Mediterranean. *Nature,* 389:473–476.

Newton, A.J., and Dugmore, A.J., 1995. Pumice: analytical report. *In* Branigan, K., and Foster, P. (Eds.), *Barra: Archaeological Research on Ben Tangaval:* Sheffield (Sheffield Univ. Press), 145–148.

Nielsen, C.H., and Sigurdsson, H., 1981. Quantitative methods for electron microprobe analysis of sodium in natural and synthetic glasses. *Am. Mineral.,* 66:547–552.

Pearce, N.J.G., Westgate, J.A., Perkins, W.T., Eastwood, W.J., and Shane, P., 1999. The application of laser ablation ICP-MS to the analysis of volcanic glass shards from tephra deposits: bulk glass and single shard analysis. *Global Planet. Change,* 21:151–171.

Potts, P.J., Tindle, A.G., and Isaacs, M.C., 1983. On the precision of electron microprobe data: a new test for the homogeneity of mineral standards. *Am. Mineral.,* 68:1237–1242.

Pouclet, A., Fujioka, K., Charvet, J., and Cadet, J.-P., 1986. Petrography and geochemistry of volcanic ash layers from Leg 87A, Nankai Trough (South Japan). *In* Kagami, H., Karig, D.E., Coulbourn, W.T., et al., *Init. Repts. DSDP,* 87: Washington (U.S. Govt. Printing Office), 695–701.

Rampino, M.R., Self, S., and Fairbridge, R.W., 1979. Can rapid climate change cause volcanic eruptions. *Science*, 206:826–829.

Robinson, S.G., 1990. Applications for whole-core magnetic susceptibility measurements of deep-sea sediments: Leg 115 results. *In* Duncan, R.A., Backman, J., Peterson, L.C., et al., *Proc. ODP, Sci. Results,* 115: College Station, TX (Ocean Drilling Program), 737–771.

Sacks, I.S., Suyehiro, K., Acton, G.D., et al., 2000. *Proc. ODP, Init. Repts.,* 186 [CD-ROM]. Available from: Ocean Drilling Program, Texas A&M University, College Station TX 77845-9547, USA.

Scientific Party, 1980. *Init. Repts. DSDP,* 56, 57: Washington (U.S. Govt. Printing Office).

Sigurdsson, H., and Loebner, B., 1981. Deep-sea record of Cenozoic explosive volcanism in the North Atlantic. *In* Self, S., and Sparks, R.S.J. (Eds.), *Tephra Studies:* Dordrecht (Reidel), 289–316.

Sigvaldason, G.E., Annertz, K., and Nilsson, M., 1992. Effect of glacier loading/deloading on volcanism: postglacial volcanic production rate of the Dyngjufjöll area, central Iceland. *Bull. Volcanol.*, 54:385–392.

Sweatman, T.R., and Long, J.V.P., 1969. Quantitative electron-probe microanalysis of rock- forming minerals. *J. Petrol.,* 10:332–379.

Westgate, J.A., and Gorton, M.P., 1981. Correlation techniques in tephra studies. *In* Self, S., and Sparks, R.S.J. (Eds), *Tephra Studies*: Dordrecht (Reidel), 73–94.

APPENDIX

Table AT1. Electron microprobe analyses of individual shards from selected tephra samples, Site 1150.

Core, section, interval (cm)/ analysis number	Major element oxide (wt%)									
	SiO_2	TiO_2	Al_2O_3	FeO	MnO	MgO	CaO	Na_2O	K_2O	Total
186-1150A-										
1H-4, 54–56										
1	73.42	0.33	12.82	1.95	0.15	0.45	2.4	3.94	1.24	96.7
2	73.92	0.35	13.11	1.92	0.09	0.58	2.37	3.79	1.11	97.24
3	74.52	0.51	12.76	2.48	0.1	0.68	2.63	2.46	1.12	97.26
4	64.48	0.3	16.47	3.95	0.42	2.1	5.71	4.56	0.61	98.6
5	72.62	0.26	12.29	1.59	0.54	0.41	2.04	2.6	1.06	93.41
6	73.59	0.58	13.13	2.09	0.1	0.56	2.51	3.2	1.38	97.14
7	75.49	0.3	12.82	1.89	0.09	0.55	2.51	2.98	1.22	97.85
8	67	1.08	13.05	5.88	0.22	1.5	4.41	2.82	0.85	96.81
9	73.06	0.4	12.16	1.51	0.59	0.38	2.14	3.28	1.28	94.8
10	73.72	0.52	11.64	2.19	0.2	0.89	1.98	3.49	1.28	95.91
11	75.96	0.34	13.35	1.56	0.12	0.38	2.38	3.58	1.5	99.17
12	73.36	0.34	10.5	1.51	0.08	0.39	1.37	2.79	1.58	91.92
13	74.38	0.32	11.38	1.44	0.09	0.33	1.36	2.74	1.41	93.45
14	72.79	0.28	12.09	1.05	0.14	0.3	1.68	3.82	1.4	93.55
15	69.42	0.29	16.92	0.74	0	0.15	4.35	5.27	0.77	97.91
16	72.16	0.17	11.43	1.25	0.5	0.32	1.65	3.89	1.33	92.7
17	70.81	0.93	14.32	3	0.18	0.75	3.94	4.32	1.36	99.61
18	72.93	0.48	14.03	2.58	0.11	0.73	3.14	3.41	1.15	98.56
19	75.16	0.33	12.52	1.62	0.06	0.46	2.17	3.88	1.17	97.37
20	74.84	0.48	12.18	1.41	0.03	0.36	1.85	3.59	1.25	95.99
21	76.22	0.22	12.02	1.46	0.09	0.35	1.9	3.83	1.4	97.49
22	73.41	0.17	11.3	1.39	0.16	0.41	1.42	1.85	2.2	92.31
23	68.99	0.26	15.94	1.22	0.08	0.42	4.11	5.62	0.85	97.49
24	73.61	0.23	12.31	1.75	0.05	0.43	2.12	3.7	1.32	95.52
25	74.94	0.36	12.52	1.75	0.07	0.45	2.05	3.98	1.54	97.66
26	75.55	0.32	12.82	1.64	0.06	0.45	2.24	3.1	1.26	97.44
27	72.81	0.27	12.1	1.46	0.19	0.43	2.05	3.62	1.22	94.15
28	73.33	0.4	13.17	2.02	0.06	0.58	2.53	3.82	1.16	97.07
29	69.78	0.32	12.36	1.73	0.09	0.5	2.29	3.31	1.12	91.5
30	71.06	0.37	12.63	1.67	0.07	0.49	2.3	3.27	0.98	92.84
31	75.43	0.3	12.37	1.41	0.11	0.38	1.9	3.61	1.32	96.83
186-1150A-										
2H-5, 136–138										
1	72.08	0.29	11.73	1.8	0.09	0.3	1.46	3.7	1.77	93.22
2	75.55	0.15	11.81	1.43	0.07	0.16	1.38	3.75	2.53	96.83
3	74.44	0.06	11.81	1.33	0.06	0.16	1.3	3.9	2.42	95.48
4	75.07	0.09	11.84	1.43	0.08	0.15	1.45	3.51	2.28	95.9
5	73.86	0.11	11.77	1.36	0.03	0.18	1.51	3.2	2.53	94.55
6	74.22	0.13	11.79	1.43	0.05	0.18	1.44	3.28	2.44	94.96
7	73.14	0.35	12.91	2.14	0.11	0.44	2.39	3.36	2.62	97.46
8	73.95	0.12	11.9	1.29	0.05	0.13	1.45	3.43	2.5	94.82
9	73.83	0.12	11.81	1.31	0.03	0.14	1.29	3.38	2.48	94.39
10	74.11	0.11	11.84	1.3	0.03	0.18	1.28	3.59	2.35	94.79
11	74.79	0.12	11.83	1.46	0.1	0.15	1.4	3.64	2.33	95.82
12	74.54	0.17	12.12	1.36	0.08	0.16	1.47	3.47	2.44	95.81
13	74.8	0.1	11.09	1.39	0.02	0.14	1.38	3.77	2.26	94.95
14	73.85	0.12	11.95	1.51	0.04	0.15	1.36	3.53	2.39	94.9
15	73.74	0.11	11.89	1.32	0.05	0.18	1.41	3.48	2.44	94.62
16	74.52	0.13	11.94	1.37	0.09	0.17	1.36	3.69	2.55	95.82
17	74.9	0.14	12	1.37	0.1	0.19	1.43	3.52	2.39	96.04
18	75.3	0.13	12.03	1.44	0.07	0.16	1.49	3.85	2.6	97.07
19	76.22	0.14	12.04	1.42	0.08	0.19	1.43	3.89	2.45	97.86
20	74.52	0.12	11.93	1.41	0.06	0.17	1.56	3.62	2.38	95.77
21	73.69	0.12	11.66	1.47	0.04	0.19	1.37	3.12	2.49	94.15
22	73.86	0.12	11.65	1.37	0.01	0.14	1.52	3.4	2.37	94.44
23	76.38	0.09	12.28	1.39	0.11	0.19	1.55	3.49	2.47	97.95
24	74.55	0.09	11.97	1.47	0	0.17	1.46	2.86	2.21	94.78
25	73.72	0.13	11.96	1.37	0.08	0.14	1.46	3.43	2.51	94.8

Note: Only a portion of this table appears here. The complete table is available in **ASCII**.

Table AT2. Electron microprobe analyses of individual shards from selected tephra samples, Site 1151.

Core, section, interval (cm)/ analysis number	Major element oxide (wt%)									
	SiO_2	TiO_2	Al_2O_3	FeO	MnO	MgO	CaO	Na_2O	K_2O	Total
186-1151C-										
2H-7, 42–44										
1	74.49	0.17	11.57	1.27	0.05	0.24	1.42	3.45	1.87	94.53
2	74.15	0.12	11.62	1.34	0.11	0.19	1.35	3.52	1.9	94.3
3	74.77	0.2	11.67	1.34	0.08	0.21	1.37	3.84	2	95.48
4	74.62	0.17	11.7	1.19	0.11	0.19	1.41	3.95	1.99	95.33
5	73.91	0.12	11.54	1.58	0.09	0.19	1.36	3.39	2.01	94.19
6	75.1	0.16	11.39	1.41	0.07	0.2	1.34	3.58	1.91	95.16
7	75.17	0.16	11.68	1.44	0.11	0.18	1.47	3.7	2.24	96.15
8	74.03	0.23	11.65	1.45	0.04	0.16	1.43	3.62	2.07	94.68
9	74.52	0.13	11.59	1.35	0.04	0.19	1.38	3.66	2.08	94.94
10	73.61	0.19	11.53	1.3	0.09	0.2	1.32	3.69	2.01	93.94
11	74.68	0.14	11.59	1.28	0.04	0.18	1.36	3.75	2.12	95.14
12	73.63	0.15	11.36	1.32	0.03	0.2	1.38	3.55	1.96	93.58
13	74.74	0.14	11.47	1.37	0.08	0.23	1.38	3.66	2.07	95.14
14	74.78	0.18	11.82	1.43	0.05	0.19	1.4	3.53	2	95.38
15	75.05	0.16	11.71	1.47	0.08	0.22	1.43	3.68	2.09	95.89
16	75.88	0.18	12.07	1.35	0.11	0.27	1.39	4.05	2.04	97.34
17	75.12	0.19	11.41	1.36	0.06	0.18	1.31	3.56	2	95.19
18	73.95	0.18	11.81	1.36	0.07	0.21	1.36	3.65	2.01	94.6
19	72.65	0.2	11.6	1.49	0.07	0.24	1.32	3.86	1.95	93.38
20	75.09	0.22	11.92	1.43	0.03	0.21	1.43	3.84	1.96	96.13
21	74.03	0.13	11.69	1.38	0.08	0.22	1.33	3.78	2.06	94.7
4H-3, 94–96										
1	73.22	0.03	12.66	1.14	0.2	0.09	0.79	3.87	1.5	93.5
2	73.07	0.03	12.64	1.2	0.18	0.11	0.76	4.2	1.63	93.82
3	72.73	0.03	12.53	1.19	0.22	0.08	0.69	3.8	1.45	92.72
4	73.34	0	12.55	1.22	0.11	0.09	0.77	3.69	1.54	93.31
5	73.84	0	12.78	1.32	0.13	0.09	0.78	3.98	1.55	94.47
6	73.09	0	12.73	1.25	0.19	0.07	0.8	3.92	1.49	93.54
7	73.2	0.05	12.78	1.31	0.15	0.07	0.77	3.97	1.51	93.81
8	73.32	0.05	12.58	1.06	0.17	0.08	0.67	4.22	1.55	93.7
9	72.97	0.07	12.48	1.24	0.14	0.17	1.14	3.93	1.36	93.5
10	73.31	0.03	12.67	1.2	0.13	0.09	0.76	3.99	1.62	93.8
11	73.06	0.04	12.73	1.13	0.14	0.06	0.7	3.69	1.52	93.07
12	73.42	0.01	12.82	1.31	0.16	0.09	0.74	4.03	1.59	94.17
13	72.62	0.02	12.55	1.18	0.09	0.06	0.72	3.61	1.53	92.38
14	73.3	0.02	12.64	1.18	0.19	0.09	0.66	3.81	1.53	93.42
15	73.21	0.03	12.47	1.1	0.14	0.09	0.69	3.71	1.46	92.9
16	72.88	0.1	11.93	1.47	0.14	0.14	1.43	3.52	1.23	92.84
5H-1, 143–145										
1	72.79	0.04	12.06	0.83	0.07	0.07	0.8	2.96	4.47	94.09
2	72.55	0.06	11.84	0.73	0.06	0.07	0.8	3.05	4.87	94.03
3	73.02	0.03	12.02	0.84	0.09	0.07	0.73	3.08	4.51	94.39
4	71.86	0	12.26	0.74	0.04	0.08	0.72	2.99	4.65	93.34
5	73.4	0.04	11.93	0.8	0.11	0.08	0.83	3.08	4.71	94.98
6	73.62	0.03	12.15	0.91	0.02	0.05	0.72	3.09	4.79	95.38
7	73.88	0.03	12.09	0.96	0.04	0.08	0.78	3.26	4.67	95.79
8	73.42	0.03	11.9	0.85	0.08	0.09	0.76	3.35	4.88	95.36
9	73.99	0.01	11.96	0.8	0.03	0.05	0.74	3.13	4.86	95.57
10	74.07	0	11.92	0.8	0.03	0.03	0.76	2.94	4.83	95.38
11	73.93	0.05	12.22	0.83	0.05	0.06	0.8	3.1	4.89	95.93
12	72.89	0.04	12.01	0.77	0.08	0.07	0.8	3.03	4.78	94.47
13	73.95	0	12.15	0.86	0.08	0.04	0.84	3.1	5.06	96.08
14	73.34	0.03	12	0.89	0.07	0.07	0.76	3.04	4.64	94.84
15	73.97	0.03	11.94	0.67	0.07	0.05	0.7	3.03	4.95	95.41
5H-4, 145–146										
1	73.18	0.16	12.48	0.99	0.02	0.22	0.88	3.52	4.14	95.59
2	72.57	0.18	12.34	0.9	0.03	0.21	0.9	3.67	3.95	94.75
3	71.52	0.25	12.21	0.88	0.06	0.26	0.9	3.39	4.15	93.62
4	72.56	0.25	12.44	0.97	0.06	0.16	0.87	3.52	3.88	94.71
5	72.69	0.2	12.47	0.94	0.06	0.2	0.85	3.51	3.98	94.9
6	71.56	0.23	12.29	0.86	0.08	0.18	0.78	3.29	4	93.27

Note: Only a portion of this table appears here. The complete table is available in **ASCII**.

Figure F1. Location map of ODP drill Sites 1150 and 1151. Contour intervals represent depth below sea level, in meters.

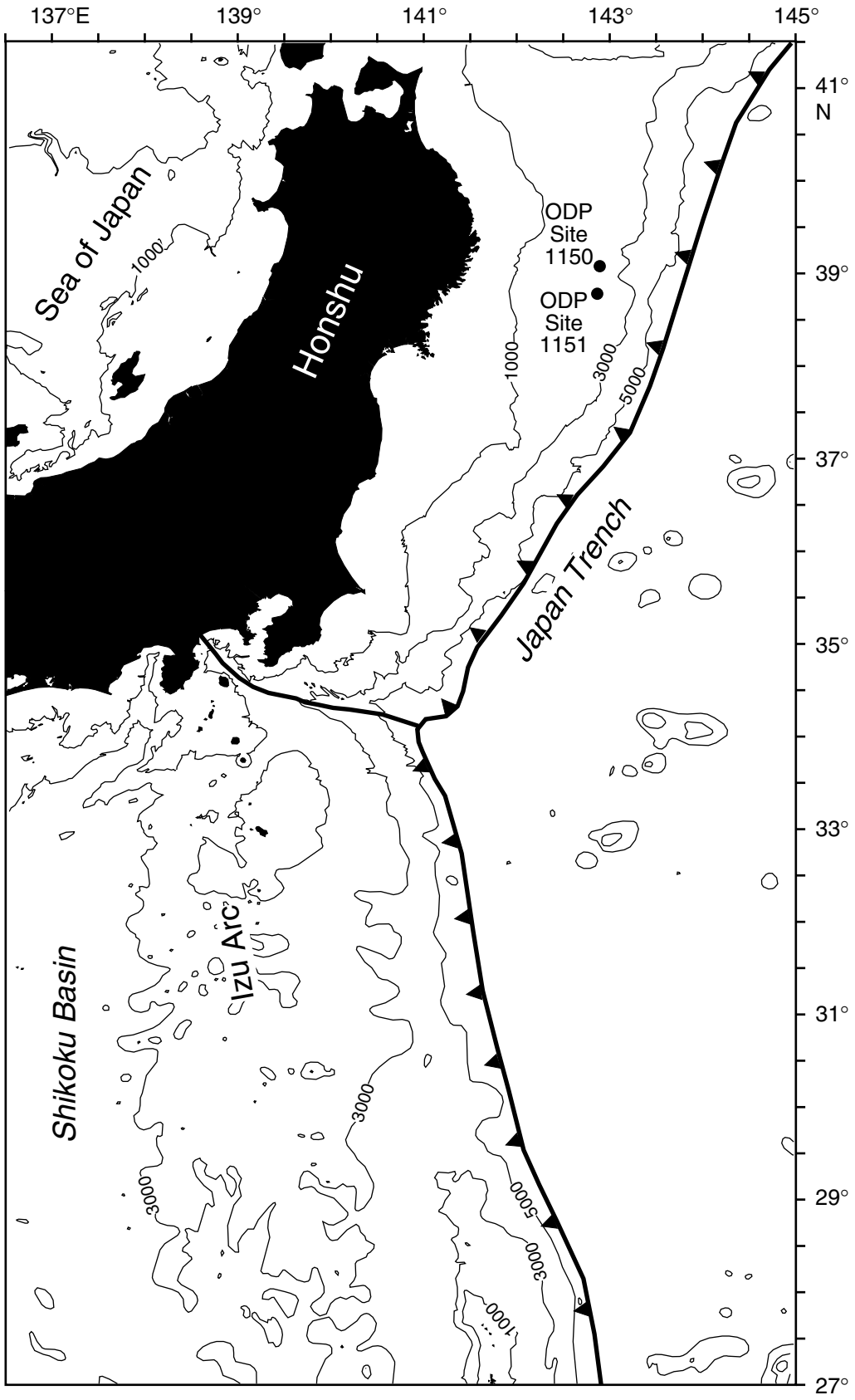

Figure F2. Proportions of volcaniclastic components in tephra pods and tephra layers from Sites 1150 and 1151.

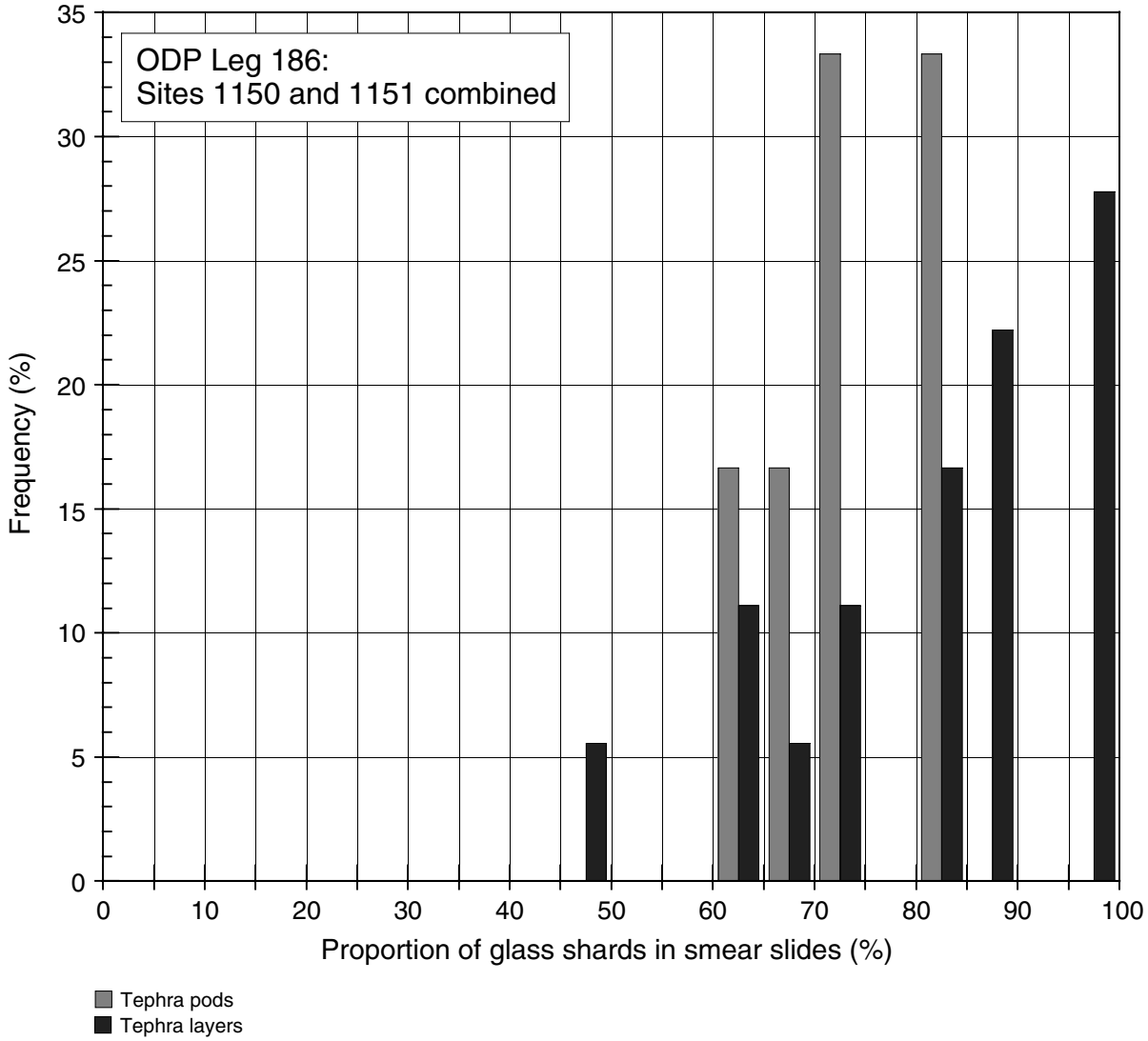

Figure F3. The range and distribution of standard deviations for specific major element oxides calculated from all analyses of individual shards within tephra layers and tephra pods at Sites 1150 and 1151, giving an indication of geochemical homogeneity. **A.** SiO_2. **B.** Al_2O_3. **C.** Na_2O. **D.** K_2O.

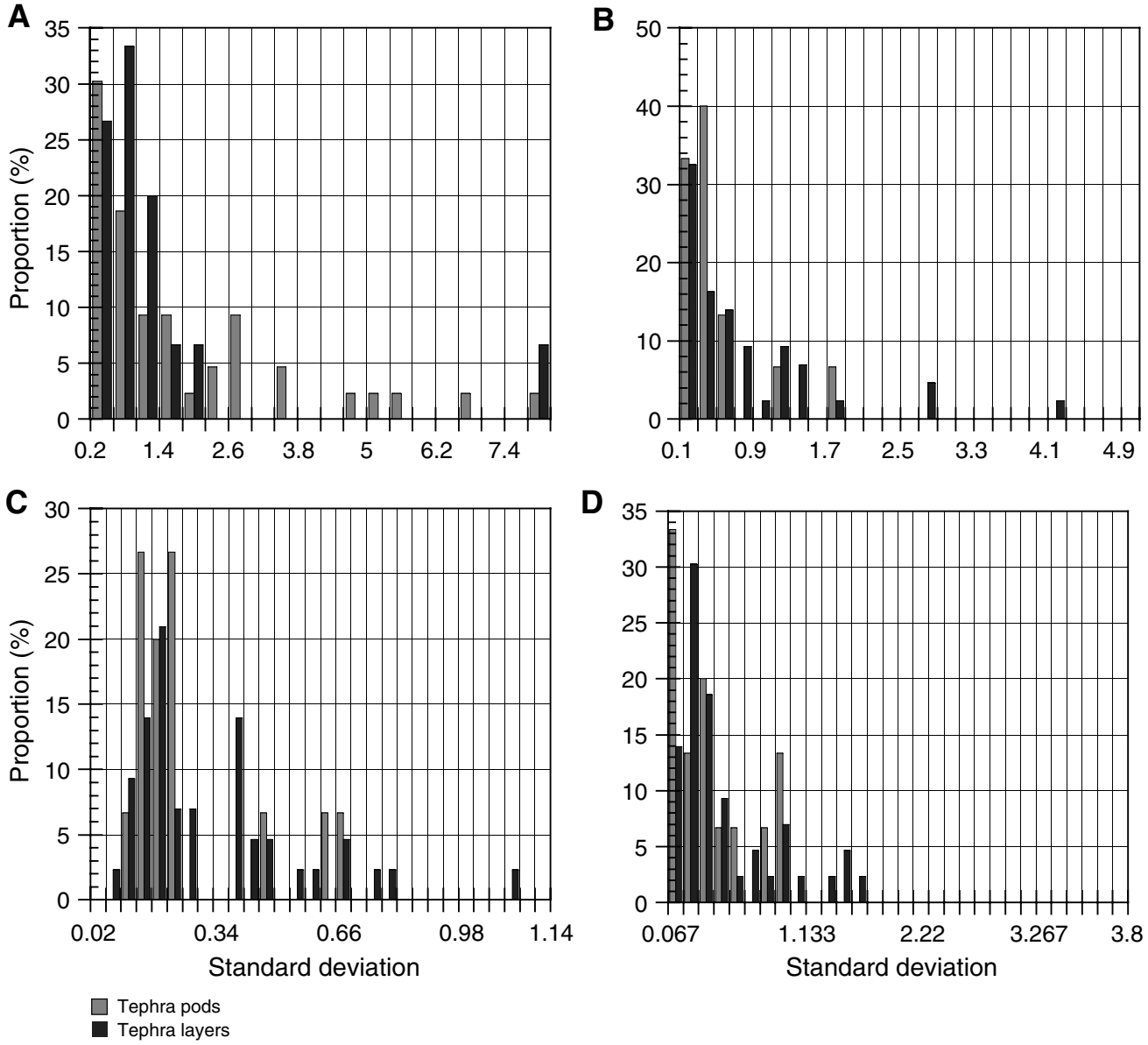

Figure F4. Decrease of total oxides in the tephra geochemical composition determined by EPMA, reflecting time-related hydration processes over approximately the last 5 m.y.

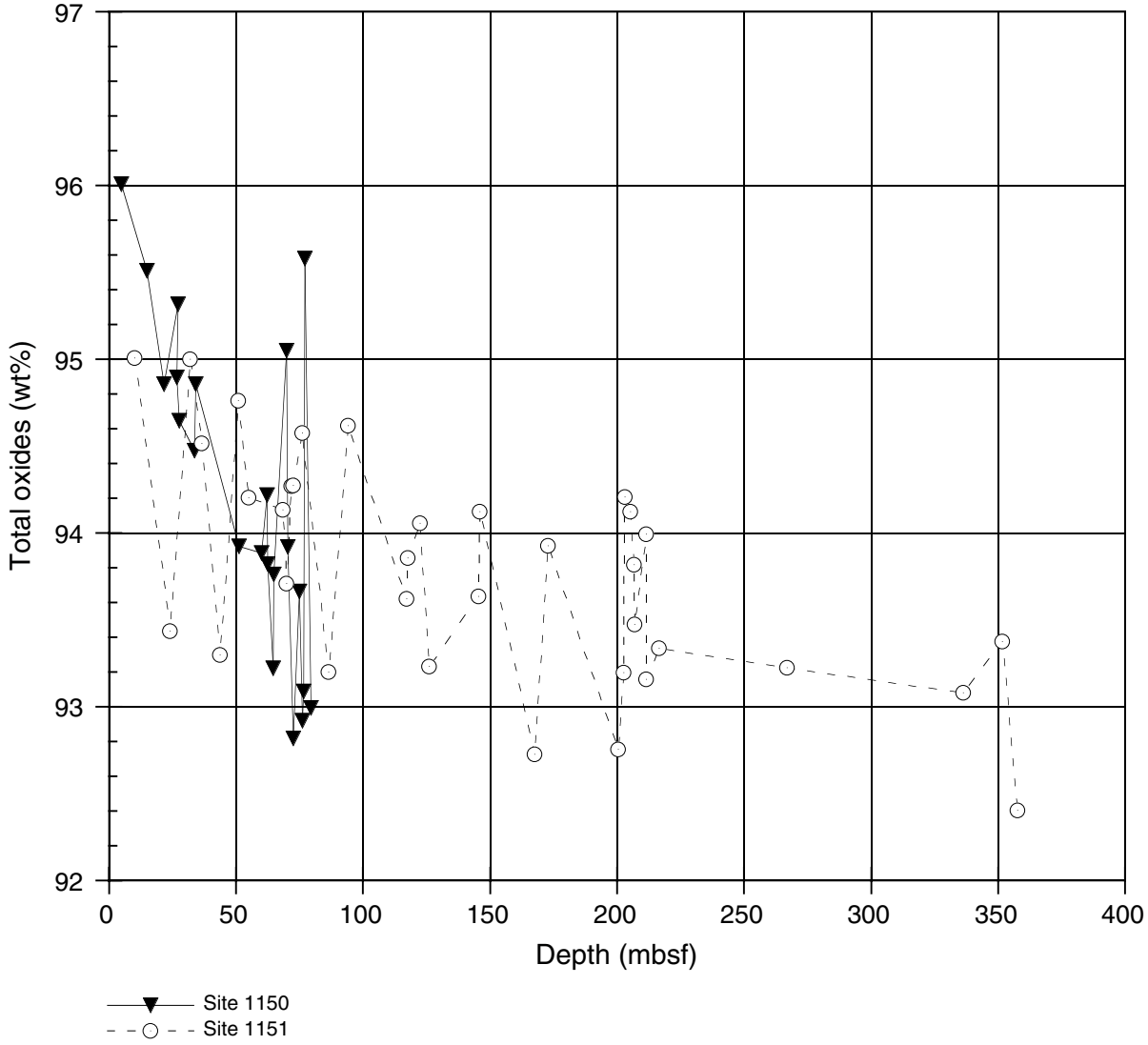

Figure F5. Lack of time-dependent signal in Al_2O_3/SiO_2 oxide ratios, indicating minimal element exchange/leaching between glass matrix and interstitial waters over approximately the last 5 m.y.

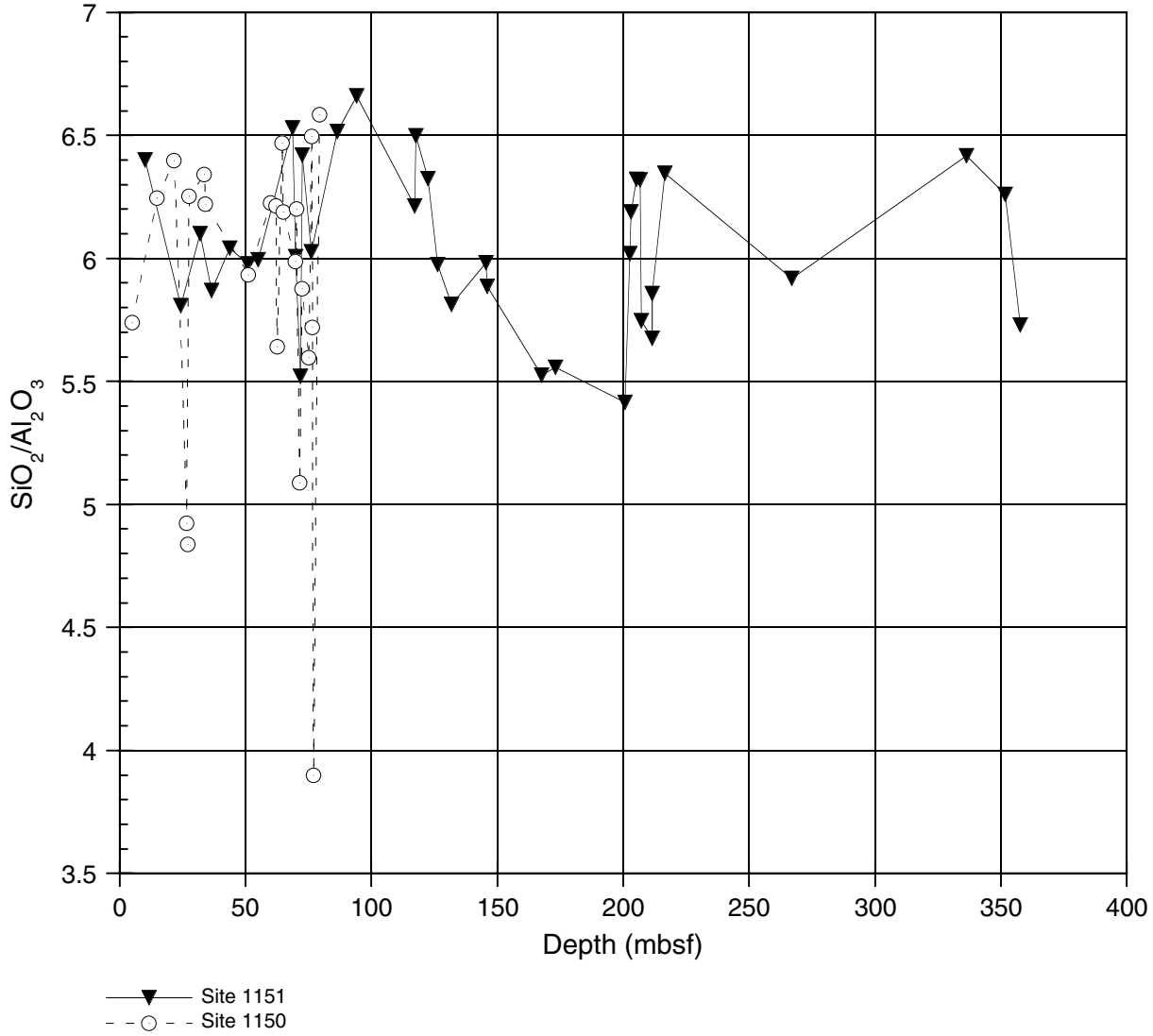

Figure F6. EPMA data for 20 of the 36 individual tephras (layers and pods) analyzed from Site 1151. These 20 tephras span an age interval, suggested by original shipboard age estimations, of ~130 ka to 4.8 Ma.

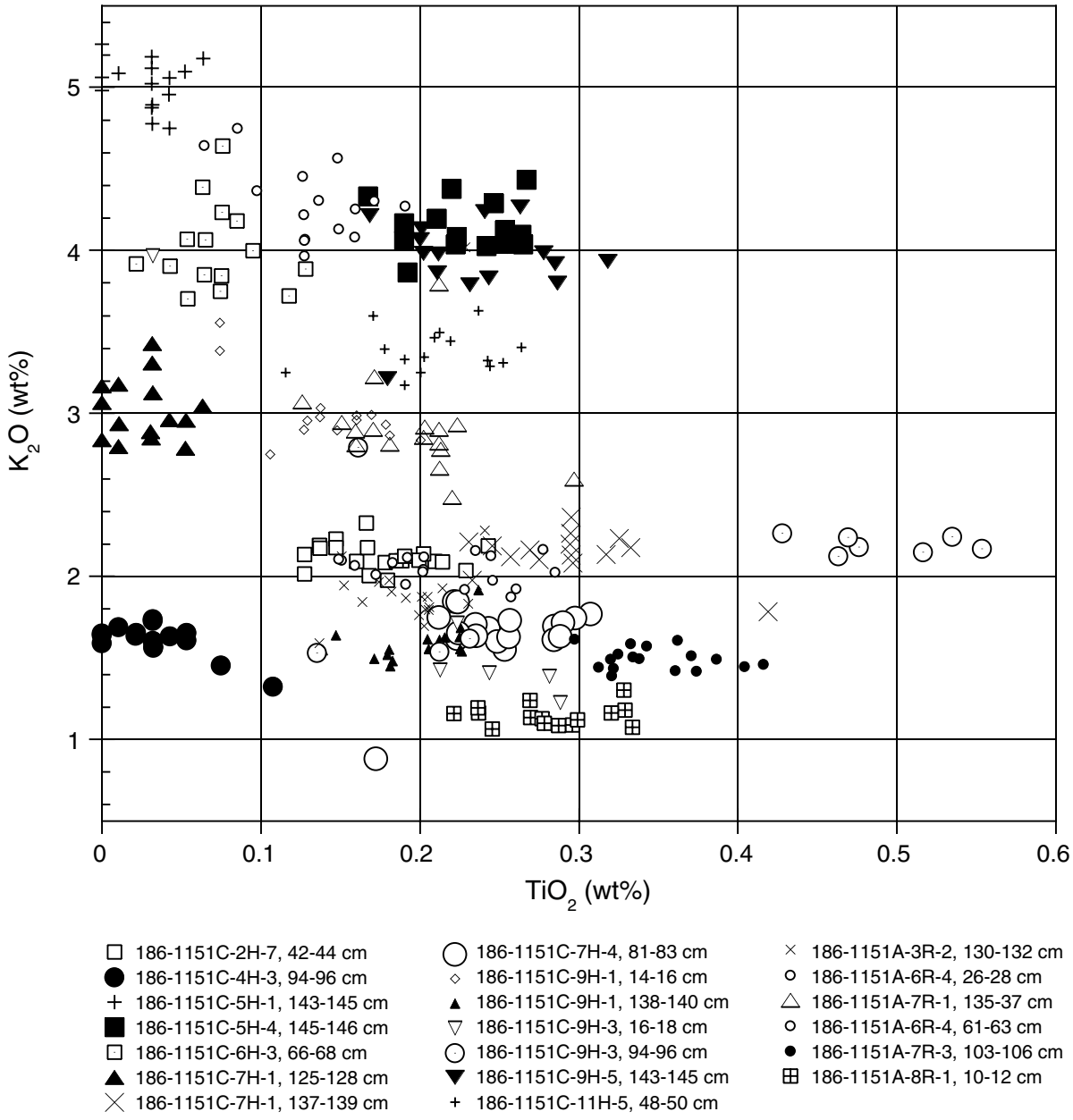

Figure F7. Geochemical comparison between tephra Sample 186-1150A-2H-5, 136–138 cm, and selected widespread late Quaternary tephras from terrestrial sites. Correlation with the ~40-ka SpFa-1 tephra erupted from the Shikotsu caldera in Hokkaido is possible. On-land and other possibly correlative marine tephra analyses depicted in this figure are taken from Cadet and Fujioka (1980), Fujioka et al. (1980), Furuta and Arai (1980a, 1980b), Machida (1999), Machida et al. (1984, 1985, 1987), and Pouclet et al. (1986).

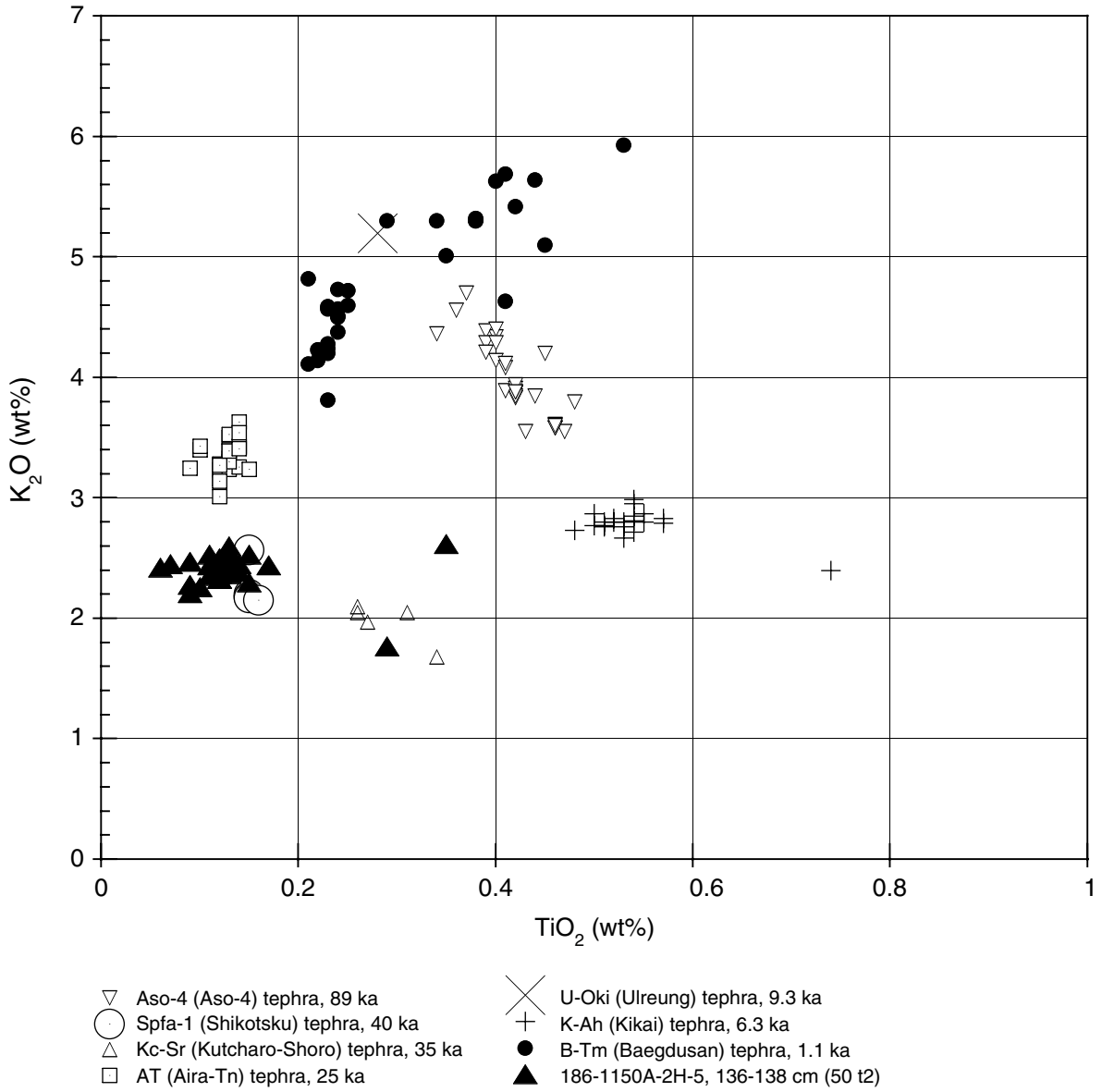

Figure F8. A, B. Comparison between selected Hole 1150A tephras and Japanese tephras dated onland or offshore between 70 and 130 ka. Tephra Samples 186-1150A-4H-1, 10–12 cm, and 3H-CC, 22–25 cm, are duplicates by core overlap and seem to be derived from the Aso volcanic system; correlation with Aso 4 and not Aso 3 is preferred because of distinct bimodality in terms of MgO, FeO*, and CaO. On-land and other possibly correlative marine tephra analyses depicted in this figure are taken from Cadet and Fujioka (1980), Fujioka et al. (1980), Furuta and Arai (1980), Machida (1999), Machida et al. (1984, 1985, 1987), and Pouclet et al. (1986).

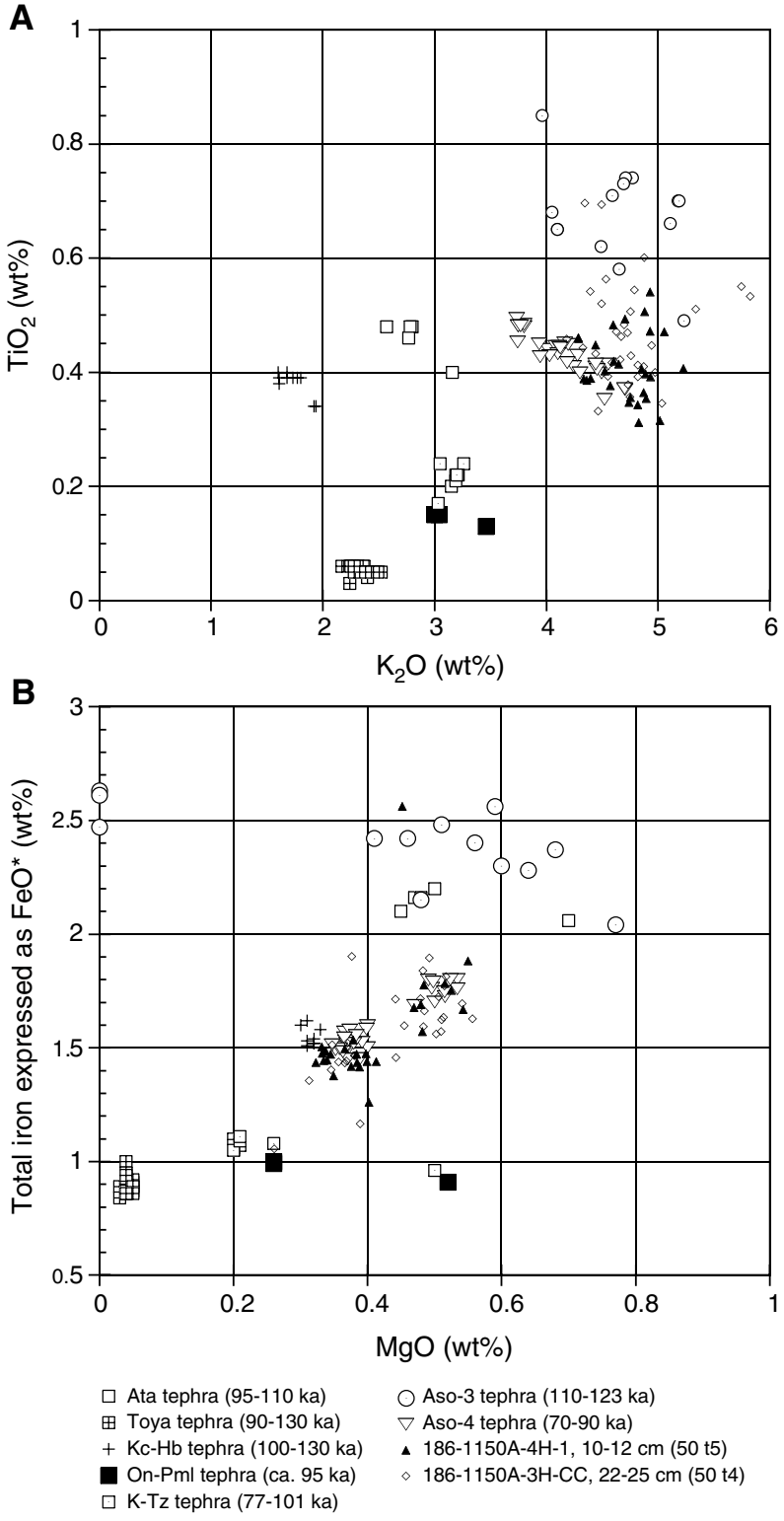

Figure F9. Comparison of tephra Sample 186-1150A-9H-3, 2–4 cm (77.22 mbsf; ~600 ka), with additional Hole 1150A tephras, tephras analyzed from Site 1151, published terrestrial tephra data from Japan, and data from Leg 87. This sample correlates with the distinctive Pouclet et al. (1986) data from Leg 87 and plots out with the main terrestrial Japanese tephras and the Ulreung field. On-land and other possibly correlative marine tephra analyses depicted in this figure are taken from Cadet and Fujioka (1980), Fujioka et al. (1980), Furuta and Arai (1980), Machida (1999), Machida et al. (1984, 1985, 1987), and Pouclet et al. (1986).

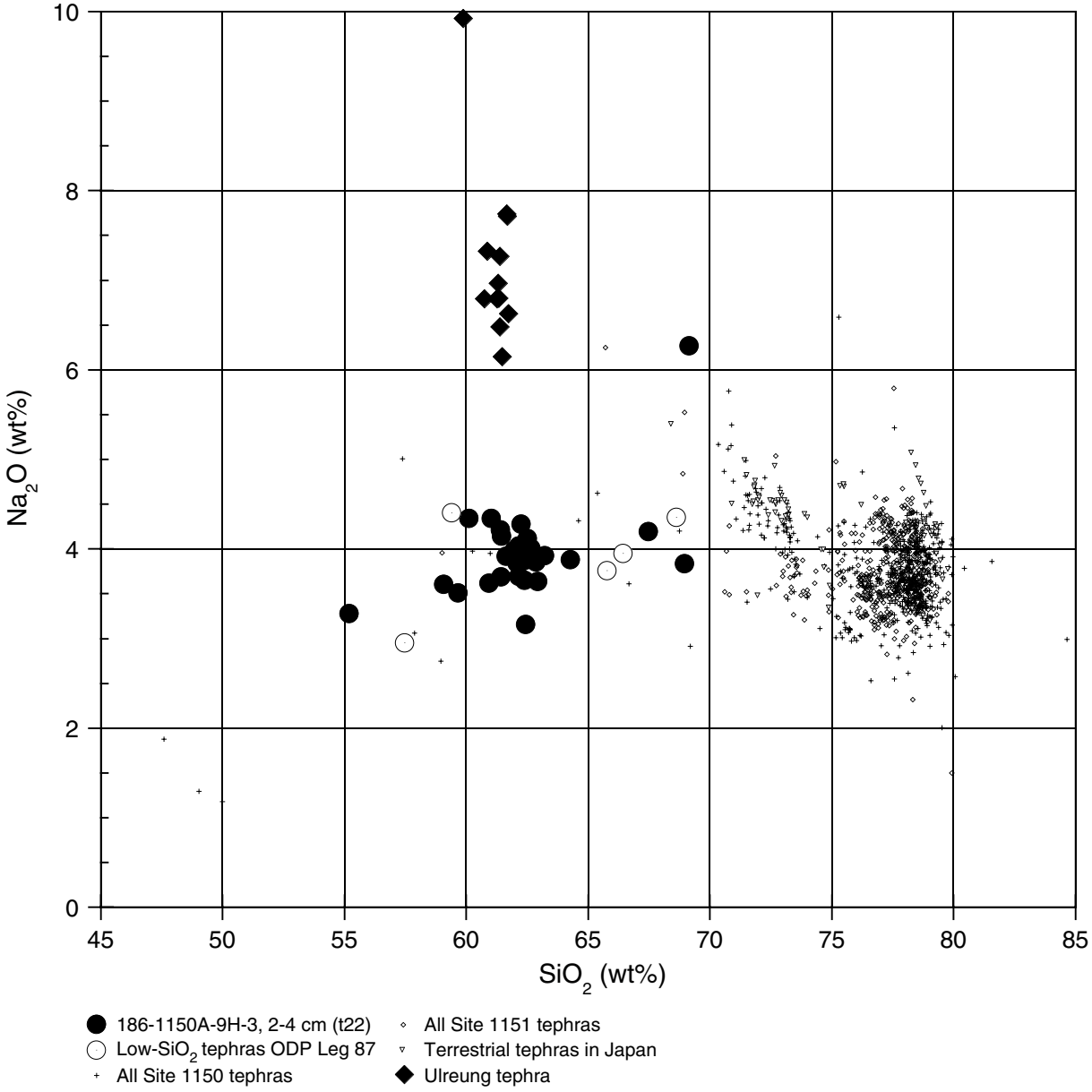

Table T1. Pliocene–Pleistocene tephra distribution and depositional style, Site 1150.

Core	Depth (mbsf)	L	P	Tephra locations
186-1150A-				
1H	0	1	1	**4:54–57,** 6:13
2H	7.7	1	1	**5:135–142,** 6:50
3H	17.2	0	3	2:140–150, **3:148–150, CC:22–25**
4H	26.7	5	3	**1:9–13,** 28–30, **110–113,** 2:90–95, 127–137, 5:45–63, **85–97, 140–146**
5H	36.2	0	4	3:145, 4:81, 6:117, 7:63
6H	45.7	2	3	3:93, 4:38–43, 95, **98–102,** 103–109
7H	55.2	10	7	2:145–150, 3:38–42, 48, 117–118, **4:30–33,** 62–63, 128, **5:100–105, 144–6:5,** 6:5–10, 15–17, 24–27, 72, 132–137, **7:50–53,** 55, 78–70
8H	64.7	5	11	1:9, 15, **36–39,** 112, 138, 3:1–4:90, **4:88–92,** 110, 115, **126–128, 5:86–90,** 127, 6:20–23, **46–52,** 83, 7:60
9H	74.2	6	1	**1:93–97, 2:60–69, 98–103, 3:0–7,** 4:3–5, **95–99,** 6:95–104
10H	83.7	2	8	3:80, 5:25–27, 91, 108–109, 135, 6:101, 125–130, 7:16–17, 7:52, CC:16
11H	93.2	7	9	1:6–8, 43–44, 104–108, 134–150, 2:0–2, 72–78, 109, 3:24–30, 99–103, 4:66–67, 5:94, 108–110, 128–134, 6:99, 7:90, 8:1–3
12H	102.7	4	6	2:40–43, 3:10–20, 82–85, 107–111, 146–4:1, 4:68–71, 5:7–12, 98, 102–112, CC:10.
13X	112.2	1	1	1:17–34, 57
14X	116.4	0	1	4:18
15X	126	1	1	2: 116–118, 130–150
16X	135.6	0	3	1:105, 2:98–100, 105–107.
17X	145.2	3	11	1:85, 2:8–9, 60, 131, 3:41, 126, 4:16, 19, 43, 5:92, 128, 6:10–11, 63–65, 7:15–16.
18X	154.8	3	2	1:2–6, 3:115–117, 4:123, 134–137, 5:89.
19X	164.4	0	0	
20X	174	0	0	
21X	183.6	1	5	2:45–47, 3:2–4, 25–33, 5:13–15, 6:4–10, 22.
22X	193.3	3	7	2:22–23, 78–79, 3:50–56, 136,148, 4:5–6, 10–14,122–123, 5:81, 6:41–42, 145–7:0.5
23X	202.9	2	5	2:26–35, 54–55, 6:9, 12–21, 7:15–20, 20–29, 79
24X	212.5	0	0	
25X	222.2	1	1	7:68–78, CC:35
26X	231.9	0	0	
27X	241.5	1	1	4:90–93, 133–137
28X	251.2	0	0	
29X	260.8	0	1	6:65–67
30X	270.4	0	0	
31X	280.1	0	0	
32X	289.7	1	5	1:110, 4:84–87, 123–129, 142–145, 4:84–87, 120–123, 123–129, 142–145, 6:28
33X	299.4	0	1	4:70–71
34X	309.1	1	0	5:47–51
35X	318.7	0	1	4:120–126
36X	328.4	0	0	
37X	338	1	1	3:48–52, 5:119–120
38X	347.6	1	0	1:146–149
39X	357.2	1	0	3:14–26
40X	366.8	1	1	1:38–41, 6:25–30
41X	376.4	1	0	1:72
42X	386	2	0	1:96–98, 7:70–72
43X	395.6	0	0	
44X	405.2	0	0	
45X	414.8	0	0	
46X	424.4	0	0	
47X	434.1	0	1	1:119–122
48X	443.7	0	1	3:96–98
49X	453.3	4	1	5:100–103, 6:133–135, 7:5–7, 17–20, 24–27
50X	462.9	0	0	
51X	472.6	0	0	

Notes: Table is based on shipboard data (Sacks, Suyehiro, Acton, et al., 2000). L = number of tephra layers, P = number of tephra pods. Analyzed results are highlighted in bold.

Table T2. Pliocene–Pleistocene tephra distribution and depositional form, Site 1151.

Core	Depth (mbsf)	L	P	Tephra locations
186-1151C-				
1H	0	0	1	1:112
2H	2.2	0	2	5:20, **6:42–44**
3H	11.7	1	2	1:40–44, 3:110–120, 6:42–44
4H	21.2	2	3	3:86–90, **92–99,** 4:36–38, 6:137–140, 7:30
5H	30.7	2	7	**1:142–150,** 2:5–10, 3:75–78, 4:43–47, 50, **144–147,** 5:7, 7:16, CC:11–14
6H	40.2	2	3	**3:64–72,** 74–78, 5:25, 57–62, 6:64–70
7H	49.7	2	4	**1:124–129,** 3:38–44, **4:80–84,** 116–124, 5:49, 124–126, CC:6–8
8H	59.2	4	4	1:19–21, 3:68–70, 4:82–85, 5:59–69, 7:18–22, 40, 79–80, CC:18–23
9H	68.7	4	8	**1:15–16, 138–140,** 2:104–110, **3:14–19,** 80, **94–96,** 4:27–29, 140–150, **5:140–150,** 6:0–2,76–78, 81–84
10H	78.2	5	3	1:27–28, 2:119–123, 133–137, 4:11–12, 15–18, 111–120, 5:68–70, 8:8–19
11H	87.7	2	4	2:46–50, 5:44, **46–54,** 6:11–15, 20–24, 117–119
186-1151A-				
3R	83.7	2	2	1:83–126, **2:129–132,** 4:90–92
4R	93.3	0	6	1:111–112, 2:10–12, 14–15, 5:17–18, 22–23, 36–38
5R	102.9	0	0	
6R	112.6	1	4	2:10–11, 83–121, 3:78–79, **4:26–28, 61–63**
7R	122.2	2	2	**1:34–38,** 2:75, 3:90, **101–105**
8R	131.8	1	2	**1:11–13,** 2:117–118, 4:8–13, 13–
9R	141.4	2	3	1:139–141, 2:148–150, **3:121–126, 4:24–26,** 66–68
10R	151	2	1	3:90–95, 5:0–4, 36–37
11R	160.6	1	5	1:93–96, 3:80–84, 91–93, 121, 4:74–77, **5:100–104**
12R	170.2	0	2	**2:132–134,** 5:59–64
13R	179.8	0	1	5:97–98
14R	189.5	1	6	4:75–85, 92–97, 100–104, 106–108, 5:37–39, 6:0–6, 7:10–11
15R	199.2	4	12	**1:145–148,** 2:0–5, **3:55–59,** 62, 88, **90–92,** 4:107–110, **5:13–18,** 42, 60–61, 89–125, **6:11–14, 17–47,** 110–111, 127–128
16R	208.9	3	6	2:36–37, **118–121,** 3:52–56, **6:30–32,** 70–71, 96–97, 99–100, 7:12–26, 40–43
17R	218.5	0	3	2:140–142, 3:105–106, 110–112.
18R	228.1	0	1	7:35–45
19R	237.70	0	1	5:85–86
20R	247.30	0	1	CC:9
21R	256.90	2	2	1:99–108, 119–120, 5:142–147, 6:116–119.
22R	266.60	2	0	**1:35–43**
23R	276.20	0	0	
24R	285.90	0	0	
25R	295.60	1	1	2:9–12, 98–108
26R	305.30	3	0	1:105–106, 106–126, 5:28–30
27R	314.90	0	4	1: 42–46, 52, 57, 62
28R	324.60	0	0	
29R	334.20	1	1	**2:68–74,** 83–87
30R	343.90	1	1	**6:30–32,** 7:12–18
31R	353.60	2	0	3:20–26, **100–103**
32R	363.20	0	1	3:56–58
33R	372.9	0	1	1:94–95
34R	382.5	0	0	
35R	392.1	0	0	

Notes: Age based on shipboard data (Sacks, Suyehiro, Acton, et al., 2000). L = number of tephra layers, P = number of tephra pods. Analyzed tephra are highlighted in bold.

Table T3. Proportions of volcanic material in tephra layers and pods.

Core, section, interval (cm)	Type	Components (%)			
		Biogenic	Siliclastic	Volcanic	Other
186-1150A-					
1H-4, 54	L	9	1	89	1
2H-5, 138	L	10	7	70	13
14X-4, 18	P	10	23	62	5
22X-6, 145	P	10	19	70	1
23X-7, 18	L	1	0	99	0
25X-7, 74	L	8	30	60	2
32X-4, 121	L	1	19	80	0
34X-5, 49	L	1	30	69	0
39X-3, 22	L	6	10	83	1
42X-1, 97	L	0	0	98	2
55X-5, 134	L	0	15	85	0
55X-5, 136	L	0	15	85	0
72X-4, 90	L	12	8	80	0
74X-5, 124	L	0	0	98	2
76X-2, 114	L	0	1	95	4
76X-3, 132	L	0	0	98	2
186-1150B-					
17R-4, 34	P	6	14	80	0
17R-4, 36	P	5	18	70	7
19R-3, 76	L	20	20	45	15
25R-3, 5	L	0	20	70	10
25R-5, 122	L	0	12	88	0
30R-4, 19	P	0	19	80	1
32R-3, 54	P	6	25	68	1
39R-4, 20	L	5	30	64	1

Notes: Data are from shipboard smear slides (Sacks, Suyehiro, Acton, et al., 2000). L = tephra layer, P = tephra pod.